

# Change in Spin State and Enhancement of Redox Reactivity of Photoexcited States of Aromatic Carbonyl Compounds by Complexation with Metal Ion Salts Acting as Lewis Acids. Lewis Acid-Catalyzed Photoaddition of Benzyltrimethylsilane and Tetramethyltin via Photoinduced Electron Transfer

Shunichi Fukuzumi,<sup>\*,†</sup> Naoya Satoh,<sup>†</sup> Toshihiko Okamoto,<sup>†</sup> Kiyomi Yasui,<sup>†</sup> Tomoyoshi Suenobu,<sup>†</sup> Yasuyo Seko,<sup>†</sup> Mamoru Fujitsuka,<sup>‡</sup> and Osamu Ito<sup>‡</sup>

Contribution from the Department of Material and Life Science, Graduate School of Engineering, Osaka University, CREST, Japan Science and Technology Corporation (JST), Suita, Osaka 565-0871, Japan, and Institute of Multidisciplinary Research for Advanced Materials, Tohoku University, CREST, Japan Science and Technology Corporation (JST), Sendai, Miyagi 980-8577, Japan

Received January 16, 2001. Revised Manuscript Received April 24, 2001

**Abstract:** The lowest excited state of aromatic carbonyl compounds (naphthaldehydes, acetonaphthones, and 10-methylacridone) is changed from the  $n,\pi^*$  triplet to the  $\pi,\pi^*$  singlet which becomes lower in energy than the  $n,\pi^*$  triplet by the complexation with metal ions such as  $\text{Mg}(\text{ClO}_4)_2$  and  $\text{Sc}(\text{OTf})_3$  ( $\text{OTf} = \text{triflate}$ ), which act as Lewis acids. Remarkable positive shifts of the one-electron reduction potentials of the singlet excited states of the Lewis acid–carbonyl complexes (e.g., 1.3 V for the 1-naphthaldehyde– $\text{Sc}(\text{OTf})_3$  complex) as compared to those of the triplet excited states of uncomplexed carbonyl compounds result in a significant increase in the redox reactivity of the Lewis acid complexes vs uncomplexed carbonyl compounds in the photoinduced electron-transfer reactions. Such enhancement of the redox reactivity of the Lewis acid complexes leads to the efficient C–C bond formation between benzyltrimethylsilane and aromatic carbonyl compounds via the Lewis-acid-promoted photoinduced electron transfer. The quantum yield determinations, the fluorescence quenching, and direct detection of the reaction intermediates by means of laser flash photolysis experiments indicate that the Lewis acid-catalyzed photoaddition reactions proceed via photoinduced electron transfer from benzyltrimethylsilane to the singlet excited states of Lewis acid–carbonyl complexes.

## Introduction

The addition of organosilane and organostannane reagents with various carbonyl compounds has been one of the most useful procedures for carbon–carbon bond formation.<sup>1,2</sup> The process requires the presence of strong Lewis acids such as  $\text{TiCl}_4$  which activate the electrophilic function of carbonyl compounds toward nucleophilic attack by the organometallic reagent controlling the acyclic stereoselection.<sup>1–4</sup> On the other hand, the photochemical carbon–carbon bond formation via photoinduced electron transfer from organometallic reagents to various

electrophiles has recently received considerable interest from both synthetic and mechanistic viewpoints.<sup>5–10</sup> However, electrophiles employed for the photoaddition by organometallic

\* To whom correspondence should be addressed: (e-mail) fukuzumi@ap.chem.eng.osaka-u.ac.jp.

<sup>†</sup> Osaka University.

<sup>‡</sup> Tohoku University.

(1) (a) Colvin, E. W. *Silicon in Organic Synthesis*; Butterworth: London, 1981. (b) Mukaiyama, T. *Angew. Chem., Int. Ed. Engl.* **1977**, *16*, 817. (c) Hosomi, A. *Acc. Chem. Res.* **1988**, *21*, 200. (d) Hoffmann, R. W. *Angew. Chem., Int. Ed. Engl.* **1987**, *26*, 489.

(2) (a) Pereyre, M.; Quitard, J.-P.; Rahm, A. *Tin in Organic Synthesis*; Butterworth: London, 1987. (b) Yamamoto, Y. *Acc. Chem. Res.* **1987**, *20*, 243.

(3) (a) Schinzer, D. *Selectivity in Lewis Acid Promoted Reactions*; Kluwer: Dordrecht, The Netherlands, 1989. (b) Shambayati, S.; Crowe, W. E.; Schreiber, S. L. *Angew. Chem., Int. Ed. Engl.* **1990**, *29*, 256.

(4) (a) Denmark, S. E.; Wilson, T. M.; Willson, T. M. *J. Am. Chem. Soc.* **1988**, *110*, 984. (b) Denmark, S. E.; Weber, E. J.; Wilson, T. M.; Willson, T. M. *Tetrahedron* **1989**, *45*, 1053. (c) Corcoran, R. C.; Ma, J. *J. Am. Chem. Soc.* **1992**, *114*, 4536. (d) Denmark, S. E.; Almstead, N. G. *J. Am. Chem. Soc.* **1993**, *115*, 3133.

(5) (a) Mariano, P. S. In *Photoinduced Electron Transfer*; Fox, M. A., Chanon, M., Eds.; Elsevier: Amsterdam, 1988; Part C, p 372. (b) Mariano, P. S. *Acc. Chem. Res.* **1983**, *16*, 130. (c) Mattes, S. L.; Farid, S. *Acc. Chem. Res.* **1982**, *15*, 80. (d) Mariano, P. S. *Synthetic Organic Chemistry*; Horspool, W. M., Ed.; Plenum Press: London, 1984. (e) Fukuzumi, S.; Tanaka, T. In *Photoinduced Electron Transfer*; Fox, M. A., Chanon, M., Eds.; Elsevier: Amsterdam, The Netherlands, 1988; Part C, p 578.

(6) (a) Ohga, K.; Mariano, P. S. *J. Am. Chem. Soc.* **1982**, *104*, 617. (b) Ohga, K.; Yoon, U. C.; Mariano, P. S. *J. Org. Chem.* **1984**, *49*, 213. (c) Mizuno, K.; Ikeda, M.; Otsuji, Y. *Tetrahedron Lett.* **1985**, *26*, 461. (d) Fukuzumi, S.; Kuroda, S.; Tanaka, T. *J. Chem. Soc., Chem. Commun.* **1986**, 1553. (e) Kubo, Y.; Imaoka, T.; Shiragami, T.; Araki, T. *Chem. Lett.* **1986**, 1749. (f) Cho, I.-S.; Tu, C.-L.; Mariano, P. S. *J. Am. Chem. Soc.* **1990**, *112*, 3594. (g) Todd, W. P.; Dinnocenzo, J. P.; Farid, S.; Goodman, J. L.; Gould, I. R. *Tetrahedron Lett.* **1993**, *34*, 2863. (h) Su, Z.; Mariano, P. S.; Falvey, D. E.; Yoon, U. C.; Oh, S. W. *J. Am. Chem. Soc.* **1998**, *120*, 10676. (i) Takahashi, Y.; Miyashi, T.; Yoon, U. C.; Oh, S. W.; Mancheno, M.; Su, Z.; Falvey, D. F.; Mariano, P. S. *J. Am. Chem. Soc.* **1999**, *121*, 3926.

(7) (a) Takuwa, A.; Tagawa, H.; Iwamoto, H.; Soga, O.; Maruyama, K. *Chem. Lett.* **1987**, 1091. (b) Takuwa, A.; Nishigaichi, Y.; Iwamoto, H. *Chem. Lett.* **1991**, 1013.

(8) (a) Sakurai, H.; Sakamoto, K.; Kira, M. *Chem. Lett.* **1984**, 1213. (b) Nakadaira, Y.; Komatsu, N.; Sakurai, H. *Chem. Lett.* **1985**, 1781. (c) Nakadaira, Y.; Sekiguchi, A.; Funada, Y.; Sakurai, H. *Chem. Lett.* **1991**, 327. (d) Mizuno, K.; Kobata, T.; Maeda, R.; Otsuji, Y. *Chem. Lett.* **1990**, 1821. (e) Fukuzumi, S.; Kitano, T.; Mochida, K. *Chem. Lett.* **1989**, 2177. (f) Fukuzumi, S.; Kitano, T.; Mochida, K. *Chem. Lett.* **1990**, 1774. (g) Fukuzumi, S.; Kitano, T.; Mochida, K. *J. Chem. Soc., Chem. Commun.* **1990**, 1236.

reagents have so far been limited to luminescent electron acceptors such as iminium cations and cyanoaromatics, which have more positive one-electron reduction potentials ( $E_{\text{red}}^0$ ) at the excited states than the one-electron oxidation potentials ( $E_{\text{ox}}^0$ ) of organometallic reagents.<sup>5–10</sup>

Since the lifetimes of excited states are usually very short and accordingly any reaction of the excited state should be fast enough to compete the decay of the excited state to the ground state, there seems to be little chance for a catalyst to accelerate further the reactions of excited states, which are already fast. There are many cases, however, such that photochemical reactions can be accelerated by some added substances which act as catalysts in the photochemical reactions.<sup>11–14</sup> The photoexcitation induces significant enhancement in the reactivity of electron transfer, and thereby photochemical reactions via photoinduced electron transfer have been reported extensively.<sup>15–20</sup> There have been some examples for photoinduced electron-transfer reactions which are catalyzed significantly,<sup>21,22</sup> since remarkable enhancement of the redox reactivity of photoexcited states of flavin analogues due to the complex formation with  $\text{Mg}(\text{ClO}_4)_2$  was first reported.<sup>23</sup> There remains a wealth of important fundamental questions with regard to catalysis in photoinduced electron transfer reactions, which has been only partially explored in the past, and which certainly deserves much more detailed attention.<sup>21,22</sup>

We report herein the first systematic studies on the change of the spin state as well as enhancement of redox reactivity of photoexcited states of aromatic carbonyl compounds due to the complexation with metal ions acting as Lewis acids.<sup>24</sup> Enhancement of fluorescence intensity has previously been reported for 2-quinolones complexed with  $\text{BF}_3$  acting as a Lewis acid.<sup>25</sup> Aromatic carbonyl compounds such as naphthaldehydes and

acetonephthones are generally nonfluorescent but phosphorescent because of the fast intersystem crossing to generate the lowest  $n, \pi^*$  triplet excited state.<sup>26</sup> However, it is found that the lowest excited state is completely changed from the  $n, \pi^*$  triplet to the  $\pi, \pi^*$  singlet which becomes lower in energy than the  $n, \pi^*$  triplet due to the complexation with metal ions such as  $\text{Mg}(\text{ClO}_4)_2$  and  $\text{Sc}(\text{OTf})_3$  ( $\text{OTf} = \text{triflate}$ ), which act as Lewis acids.<sup>27</sup> Efficient photoaddition of benzyltrimethylsilane ( $\text{PhCH}_2\text{-SiMe}_3$ ) with aromatic carbonyl compounds is made possible by the complexation of the photoexcited states with metal ions.<sup>24</sup> The catalytic mechanism for the photoaddition reaction is revealed on the basis of the studies done on the complex formation between carbonyl compounds and Lewis acids, the quantum yield determinations, the fluorescence quenching by electron donors, and direct detection of the reaction intermediates by means of laser flash photolysis experiments.

## Experimental Section

**Materials.** 1-Naphthaldehyde (1-NA), 2-naphthaldehyde (2-NA), 1-acetonephthone (1-AN), 2-acetonephthone (2-AN), 10-methylacridone, and alkylbenzene derivatives were obtained commercially and purified by the standard method.<sup>28</sup> Benzyltrimethylsilane, trimethylsilyl trifluoromethanesulfonate, and tetramethyltin were also obtained commercially and used as received. A dimeric 1-benzyl-1,4-dihydroquinolinamide [(BNA)<sub>2</sub>] was prepared according to the literature.<sup>29</sup> Scandium triflate [ $\text{Sc}(\text{OTf})_3$ ] was prepared by the following procedure according to the literature.<sup>30</sup> A deionized aqueous solution was mixed (1:1 v/v) with trifluoromethanesulfonic acid (>99.5%, 10.6 mL) obtained from the Central Glass, Co., Ltd., Japan. The trifluoromethanesulfonic acid solution was slowly added to a flask which contained scandium oxide ( $\text{Sc}_2\text{O}_3$ ) (>99.9%, 30 mmol) obtained from Shin Etsu Chemical, Co., Ltd., Japan. The mixture was refluxed at 100 °C for 3 days. After centrifugation of the reaction mixture, the solution containing scandium triflate was separated and water was removed by vacuum evaporation for 40 h. Similarly, lutetium triflate and ytterbium triflate were prepared by the reaction of lutetium oxide and ytterbium oxide with an aqueous solution of trifluoromethanesulfonic acid. Lanthanum triflate was obtained from Aldrich as the hexahydrate form and used after drying under vacuum evacuation for 40 h. Magnesium triflate [ $\text{Mg}(\text{OTf})_2$ ] was obtained from Aldrich and used as received. Anhydrous magnesium perchlorate [ $\text{Mg}(\text{ClO}_4)_2$ ] was obtained from Nacalai Tesque. Potassium ferrioxalate used as an actinometer was prepared according to the literature,<sup>31</sup> and purified by recrystallization from hot water. Tetrabutylammonium hexafluorophosphate used as a supporting electrolyte for the electrochemical measurements was obtained commercially and purified by the standard method.<sup>28</sup> Acetonitrile, propionitrile and dichloromethane as solvents were purified and dried by the standard procedure.<sup>28</sup> Acetonitrile-*d*<sub>3</sub> was obtained from EURI SO-TOP, CEA, France.

**Reaction Procedures.** Photoaddition of benzyltrimethylsilane with aromatic carbonyl compounds was performed in the presence of Mg-

(9) (a) Fukuzumi, S.; Fujita, M.; Otera, J.; Fujita, Y. *J. Am. Chem. Soc.* **1992**, *114*, 10271. (b) Fukuzumi, S.; Fujita, M.; Otera, J. *J. Org. Chem.* **1993**, *58*, 5405. (c) Mikami, K.; Matsumoto, S.; Ishida, A.; Takamuku, S.; Suenobu, T.; Fukuzumi, S. *J. Am. Chem. Soc.* **1995**, *117*, 11134. (d) Mikami, K.; Matsumoto, S.; Okubo, Y.; Fujitsuka, M.; Ito, O.; Suenobu, T.; Fukuzumi, S. *J. Am. Chem. Soc.* **2000**, *122*, 2236.

(10) For thermal electron-transfer reactions involving main-group organometallics, see: (a) Kaim, W. *Acc. Chem. Res.* **1985**, *18*, 160. (b) Kochi, J. K. *Angew. Chem., Int. Ed. Engl.* **1988**, *27*, 1227.

(11) (a) Wubbels, G. G. *Acc. Chem. Res.* **1983**, *16*, 285. (b) Wubbels, G. G.; Celander, D. W. *J. Am. Chem. Soc.* **1981**, *103*, 7669.

(12) Albini, A. *J. Chem. Educ.* **1986**, *63*, 383.

(13) (a) *Photocatalysis, Fundamentals and Applications*; Serpone, N., Pelizzetti, E., Eds.; Wiley: New York, 1989. (b) *Homogeneous Photocatalysis*; Chanon, M., Ed.; Wiley: Chichester, UK, 1997.

(14) (a) Lewis, F. D.; Howard, D. K.; Oxman, J. D. *J. Am. Chem. Soc.* **1983**, *105*, 3344. (b) Lewis, F. D.; Oxman, J. D. *J. Am. Chem. Soc.* **1984**, *106*, 466. (c) Lewis, F. D.; Oxman, J. D.; Gibson, L. L.; Hampsch, H. L.; Quillen, S. L. *J. Am. Chem. Soc.* **1986**, *108*, 3005. (d) Lewis, F. D.; Howard, D. K.; Oxman, J. D.; Uphagrove, A. L.; Quillen, S. L. *J. Am. Chem. Soc.* **1986**, *108*, 5964. (e) Lewis, F. D.; Quillen, S. L.; Hale, P. D.; Oxman, J. D. *J. Am. Chem. Soc.* **1988**, *110*, 1261. (f) Lewis, F. D.; Barancyk, S. V. *J. Am. Chem. Soc.* **1989**, *111*, 8653. (g) Lewis, F. D.; Elbert, J. E.; Uphagrove, A. L.; Hale, P. D. *J. Org. Chem.* **1991**, *56*, 553. (h) Lewis, F. D.; Barancyk, S. V.; Burch, E. L. *J. Am. Chem. Soc.* **1992**, *114*, 3866.

(15) Fox, M. A.; Chanon, M., Eds. *Photoinduced Electron Transfer*; Elsevier: Amsterdam, The Netherlands, 1988; Parts A–D.

(16) Julliard, M.; Chanon, M. *Chem. Rev.* **1983**, *83*, 425.

(17) Kavarnos, G. J.; Turro, N. J. *Chem. Rev.* **1986**, *86*, 401.

(18) Müller, F.; Mattay, J. *Chem. Rev.* **1993**, *93*, 99.

(19) Rathore, R.; Kochi, J. K. *Adv. Phys. Org. Chem.* **2000**, *35*, 193.

(20) Ho, T.-I.; Ho, J.-H.; Wu, J.-Y. *J. Am. Chem. Soc.* **2000**, *122*, 8575.

(21) Fukuzumi, S.; Itoh, S. In *Advances in Photochemistry*; Neckers, D. C., Volman, D. H., von Bünnau, G., Eds.; John Wiley & Sons: New York, 1999; Vol. 25, p 107.

(22) Fukuzumi, S. In *Electron Transfer in Chemistry*; Balzani, V., Ed.; Wiley-VCH: Weinheim, Germany, 2001; Vol. 4, pp 3–67.

(23) (a) Fukuzumi, S.; Kuroda, S.; Tanaka, T. *J. Am. Chem. Soc.* **1985**, *107*, 3020. (b) Fukuzumi, S.; Kuroda, S.; Tanaka, T. *Chem. Lett.* **1984**, 417.

(24) A preliminary report has appeared: Fukuzumi, S.; Okamoto, T.; Otera, J. *J. Am. Chem. Soc.* **1994**, *116*, 5503.

(25) Lewis, F. D.; Reddy, G. D.; Elbert, J. E.; Tillberg, B. E.; Meltzer, J. A.; Kojima, M. *J. Org. Chem.* **1991**, *56*, 5311.

(26) Turro, N. J. *Molecular Photochemistry*; W. A. Benjamin, Inc.: New York, 1967.

(27) Heavy metal cations in zeolites have been reported to accelerate spin-state interconversion (singlet–triplet intersystem crossing) of excited guest molecules. See: (a) Ramamurthy, V.; Caspar, J. V.; Eaton, D. F.; Kuo, E. W.; Corbin, D. R. *J. Am. Chem. Soc.* **1992**, *114*, 3882. (b) Uppilli, S.; Marti, V.; Nikolaus, A.; Jockusch, S.; Adam, W.; Engel, P. S.; Turro, N. J.; Ramamurthy, V. *J. Am. Chem. Soc.* **2000**, *122*, 11025.

(28) Perrin, D. D.; Armarego, W. L. F. *Purification of Laboratory Chemicals*; Butterworth-Heinemann: Oxford, England, 1988.

(29) Wallenfels, K.; Gellerich, M. *Chem. Ber.* **1959**, *92*, 1406.

(30) (a) Forsberg, J. H.; Spaziano, V. T.; Balasubramanian, T. M.; Liu, G. K.; Kinsley, S. A.; Duckworth, C. A.; Poteruca, J. J.; Brown, P. S.; Miller, J. L. *J. Org. Chem.* **1987**, *52*, 1017. (b) Kobayashi, S.; Hachiya, I. *J. Org. Chem.* **1994**, *59*, 3590. (c) Kobayashi, S.; Hachiya, I.; Ishitani, H.; Araki, M. *Synlett* **1993**, 472.

(31) (a) Hatchard, C. G.; Parker, C. A. *Proc. R. Soc. London, Ser. A* **1956**, *235*, 518. (b) Calvert, J. G.; Pitts, J. N. *Photochemistry*; Wiley: New York, 1966; p 783.

(ClO<sub>4</sub>)<sub>2</sub> in MeCN. Typically, benzyltrimethylsilane (1.0 × 10<sup>-1</sup> M) was added by means of a microsyringe to a CD<sub>3</sub>CN solution (0.7 mL) containing 2-NA (5.0 × 10<sup>-2</sup> M) and Mg(ClO<sub>4</sub>)<sub>2</sub> (2.0 × 10<sup>-1</sup> M) in a square quartz cuvette (1 mm i.d.) and the solution was deaerated by bubbling with argon gas for 5 min. The solution was irradiated with monochromatized light from a xenon lamp of a Shimadzu RF-5000 spectrofluorophotometer for 6.5 h. The experimental details for other photochemical reactions are given in the Supporting Information (S1). The products were identified by comparison of the <sup>1</sup>H NMR spectra with those of the authentic samples.<sup>24,32</sup> No homo-coupling products such as dibenzyl have been detected. The isolated yield was 70%. <sup>1</sup>H NMR measurements were performed with a Japan Electron Optics JNM-GSX-400 (400 MHz) NMR spectrometer at 298 K. <sup>1</sup>H NMR (CD<sub>3</sub>CN, 298 K) δ (Me<sub>4</sub>Si, ppm): (C<sub>10</sub>H<sub>7</sub>[2-CH(CH<sub>2</sub>Ph)(OSiMe<sub>3</sub>)] 0.14 (s, 9H), 3.13 (dd, 1H, *J* = 13.9, 6.1 Hz), 3.15 (dd, 1H, *J* = 13.9, 7.6 Hz) 5.05–5.11 (m, 1H), 7.14–7.22 (m, 5H), 7.46–7.58 (m, 3H), 7.79–7.92 (m, 4H); (C<sub>10</sub>H<sub>7</sub>[1-CH(CH<sub>2</sub>Ph)(OSiMe<sub>3</sub>)]), 65%) 0.14 (s, 9H), 3.11 (dd, 1H, *J* = 13.9, 8.4 Hz), 3.24 (dd, 1H, *J* = 13.9, 4.6 Hz), 5.67–5.72 (m, 1H), 7.26–7.33 (m, 5H), 7.50–8.26 (m, 7H); (C<sub>10</sub>H<sub>7</sub>[2-CMe(CH<sub>2</sub>Ph)(OSiMe<sub>3</sub>)]), 72%) 0.14 (s, 9H), 1.62 (s, 3H), 3.15, 3.20 (ABq, 2H, *J* = 13.2 Hz), 7.14–7.19 (m, 5H), 7.46–7.52 (m, 3H), 7.82–7.90 (m, 4H); (C<sub>10</sub>H<sub>7</sub>[1-CMe(CH<sub>2</sub>Ph)(OSiMe<sub>3</sub>)]), 32%) 0.17 (s, 9H), 1.76 (s, 3H), 3.46 (s, 2H), 7.34–7.44 (m, 5H), 7.54–8.12 (m, 7H); (C<sub>10</sub>H<sub>7</sub>[1-CH(Me)(OSnMe<sub>3</sub>)]), 100%) 0.21 (s, 9H), 1.09 (d, 3H, *J* = 4.6 Hz), 4.97 (m, 1H), 7.16–7.27 (m, 4H), 7.56–7.77 (m, 3H); (Acr-(CH<sub>2</sub>Ph)<sup>+</sup>, 100%) 4.79 (s, 3H), 5.35 (s, 2H), 8.9–7.5 (m, 13H).

**Spectral Measurements.** The formation of metal ion complexes with naphthaldehydes and acetophenones was examined from the change in the UV–vis spectra in the presence of various concentrations of metal ions (M<sup>n+</sup>) by using a Hewlett-Packard 8452A diode array spectrophotometer. The formation constants were determined from linear plots of (A – A<sub>0</sub>)<sup>-1</sup> vs [M<sup>n+</sup>]<sup>-1</sup>, where A and A<sub>0</sub> are the absorbance at λ<sub>max</sub> in the presence of the metal ion and the absorbance at the same wavelength in the absence of the metal ion, respectively.

**Quantum Yield Determinations.** A standard actinometer (potassium ferrioxalate)<sup>31</sup> was used for the quantum yield determinations. In the case of photoaddition of PhCH<sub>2</sub>SiMe<sub>3</sub> with aromatic carbonyl compounds, an MeCN solution (3.0 mL) containing an aromatic carbonyl compound (5.1 × 10<sup>-4</sup> – 1.0 × 10<sup>-3</sup> M), PhCH<sub>2</sub>SiMe<sub>3</sub> (7.1 × 10<sup>-3</sup> to 1.7 × 10<sup>-1</sup> M), and Mg(ClO<sub>4</sub>)<sub>2</sub> (1.0 M) in a square quartz cuvette (10 mm i.d.) was deaerated thoroughly with a stream of argon for 7 min, and it was irradiated with monochromatized light of λ = 340 nm from a Shimadzu RF-5000 fluorescence spectrophotometer with the slit width of 20 nm. Under the conditions of actinometry experiments, both the actinometer and aromatic carbonyl compounds absorbed essentially all the incident light of λ = 340 nm. The light intensity of monochromatized light of λ = 340 nm was determined as 7.98 × 10<sup>-6</sup> einstein dm<sup>-3</sup> s<sup>-1</sup> with the slit width of 20 nm. The photochemical reaction was monitored using a Hewlett-Packard 8452A diode-array spectrophotometer. The quantum yields for the photoaddition of benzyltrimethylsilane to 2-NA, 1-NA, 2-AN, and 1-AN in the presence of Mg(ClO<sub>4</sub>)<sub>2</sub> (1.0 M) in deaerated MeCN were determined from the decrease in absorbance at λ = 346 nm (ε = 2.3 × 10<sup>3</sup> M<sup>-1</sup> cm<sup>-1</sup>), λ = 350 nm (ε = 3.7 × 10<sup>3</sup> M<sup>-1</sup> cm<sup>-1</sup>), λ = 342 nm (ε = 1.9 × 10<sup>3</sup> M<sup>-1</sup> cm<sup>-1</sup>), and λ = 350 nm (ε = 1.1 × 10<sup>3</sup> M<sup>-1</sup> cm<sup>-1</sup>), respectively. The detailed procedures for other photochemical reactions are given in the Supporting Information (S1–S2).

**Fluorescence Quenching.** Quenching experiments of the fluorescence of metal ion complexes of aromatic carbonyl compounds were carried out by using a Shimadzu spectrofluorophotometer (RF-5000). The excitation wavelengths for 2-NA, 1-NA, 2-AN, and 1-AN were 375, 375, 370, and 350 nm in the presence of Mg(ClO<sub>4</sub>)<sub>2</sub> (1.0 M) in deaerated MeCN, respectively. The excitation wavelength for 1-NA in the presence of Sc(OTf)<sub>3</sub> (1.0 × 10<sup>-2</sup> M) was 380 nm in deaerated MeCN. The monitoring wavelengths were those corresponding to the maxima of the emission bands. The excitation wavelength of AcrCO–Sc(OTf)<sub>3</sub> and AcrCO–Me<sub>3</sub>SiOTf was 413 nm in MeCN and CH<sub>2</sub>Cl<sub>2</sub>. The monitoring wavelength was corresponding to the maximum of the

emission band at λ<sub>max</sub> = 474 nm. The MeCN solutions were deaerated by argon purging for 7 min prior to the measurements. Relative fluorescence intensities were measured for MeCN solutions containing an aromatic carbonyl compound (2.0 × 10<sup>-4</sup> M) with a quencher at various concentrations in the presence of 1.0 M Mg(ClO<sub>4</sub>)<sub>2</sub>. Relative fluorescence intensities were measured for MeCN solutions containing 1-NA (3.0 × 10<sup>-4</sup> M) with various alkylbenzenes (1.0 × 10<sup>-2</sup> to 9.6 × 10<sup>-1</sup> M) in the presence of metal ions (Sc(OTf)<sub>3</sub>, 1.0 × 10<sup>-2</sup> M; Mg(ClO<sub>4</sub>)<sub>2</sub>, 1.0 × 10<sup>-1</sup> M). Relative fluorescence intensities were also measured for an MeCN solution containing AcrCO–Sc(OTf)<sub>3</sub> (5.0 × 10<sup>-5</sup> M) with various electron donors (2.0 × 10<sup>-3</sup> to 7.0 × 10<sup>-1</sup> M) in the presence of Sc(OTf)<sub>3</sub> 8.0 × 10<sup>-3</sup> to 8.0 × 10<sup>-2</sup> M or a CH<sub>2</sub>Cl<sub>2</sub> solution containing AcrCO–Me<sub>3</sub>SiOTf (1.0 × 10<sup>-4</sup> M) with various electron donors (1.9 × 10<sup>-3</sup> to 7.7 × 10<sup>-1</sup> M) in the presence of Me<sub>3</sub>SiOTf (2.0 × 10<sup>-3</sup> M). There was no change in the shape but there was a change in the intensity of the fluorescence spectrum by the addition of a quencher. The Stern–Volmer relationship (eq 1) was obtained for the ratio of the fluorescence intensities (I<sub>0</sub>/I) in the absence

$$I_0/I = 1 + K_q[D] \quad (1)$$

and presence of electron donors and the concentrations of donors used as quenchers [D]. The fluorescence lifetimes (τ) of the metal ion complexes of aromatic carbonyl compounds were determined in deaerated MeCN and CH<sub>2</sub>Cl<sub>2</sub> at 298 K by single photon counting using a Horiba NAES-1100 time-resolved spectrofluorophotometer. The observed quenching rate constants k<sub>q</sub> (= K<sub>q</sub>τ<sup>-1</sup>) were obtained from the K<sub>q</sub> and τ values.

**Electrochemical Measurements.** Electrochemical measurements were performed on a BAS 100B electrochemical analyzer in deaerated MeCN containing 0.10 M n-Bu<sub>4</sub>N<sup>+</sup>PF<sub>6</sub><sup>-</sup> (TBAPF<sub>6</sub>) as a supporting electrolyte at 298 K. The platinum working electrode was polished with BAS polishing alumina suspension and rinsed with acetone before use. The counter electrode was a platinum wire. The measured potentials were recorded with respect to an Ag/AgNO<sub>3</sub> (0.01 M) reference electrode. The second-harmonic alternating current voltammetry (SHACV)<sup>33</sup> measurements of alkylbenzenes, 2-NA, 1-NA, AcrCO, and the AcrCO–Sc(OTf)<sub>3</sub> complex were carried out with a BAS 100B electrochemical analyzer in deaerated MeCN containing 0.10 M TBAPF<sub>6</sub> as a supporting electrolyte at 298 K. The E<sup>0</sup><sub>red</sub> values (vs Ag/AgNO<sub>3</sub>) are converted into those vs SCE by addition of 0.29 V.<sup>34</sup>

**Laser Flash Photolysis.** Triplet–triplet transient absorption spectra of 1-NA and 1-NA–Mg(ClO<sub>4</sub>)<sub>2</sub> complexes were measured by laser flash photolysis of the MeCN solution containing 1-NA (1.0 × 10<sup>-3</sup> M) in the absence and presence of Mg(ClO<sub>4</sub>)<sub>2</sub> (1.0 M), respectively. To observe transient absorption spectra in the photochemical reaction of the 1-NA–Mg(ClO<sub>4</sub>)<sub>2</sub> complex with PhCH<sub>2</sub>SiMe<sub>3</sub>, a deaerated MeCN solution containing 1-NA (2.8 × 10<sup>-4</sup> M), PhCH<sub>2</sub>SiMe<sub>3</sub> (1.7 × 10<sup>-1</sup> M), and Mg(ClO<sub>4</sub>)<sub>2</sub> (1.0 M) was excited by a Nd:YAG laser (Continuum, Surelite II-10) at 355 nm with the power of 15 mJ at 298 K. For the detection of transient absorption spectra in the photochemical reaction of the AcrCO–Sc(OTf)<sub>3</sub> complex with PhCH<sub>2</sub>SiMe<sub>3</sub>, a deaerated MeCN solution containing AcrCO (1.0 × 10<sup>-4</sup> M), PhCH<sub>2</sub>SiMe<sub>3</sub> (2.5 × 10<sup>-1</sup> M), and Sc(OTf)<sub>3</sub> (8.0 × 10<sup>-2</sup> M) was excited by an optical parametric oscillation (Continuum Surelite OPO, fwhm 4 ns, 440 nm) pumped by a Nd:YAG laser (Continuum, Surelite II-10) with the power of 10 mJ. For the photoinduced electron transfer from (BNA)<sub>2</sub> to the 1-NA–Mg(ClO<sub>4</sub>)<sub>2</sub> complex and the AcrCO–Sc(OTf)<sub>3</sub> complex, (BNA)<sub>2</sub> (2.0 × 10<sup>-4</sup> M) was employed in place of PhCH<sub>2</sub>SiMe<sub>3</sub> under otherwise the same experimental conditions. The transient spectra were recorded using fresh solutions in each laser excitation.

(33) The SHACV method provides a superior approach to directly evaluating the one-electron redox potentials in the presence of a follow-up chemical reaction, relative to the better-known dc and fundamental harmonic ac methods. See: (a) McCord, T. G.; Smith, D. E. *Anal. Chem.* **1969**, *41*, 1423. (b) Bond, A. M.; Smith, D. E. *Anal. Chem.* **1974**, *46*, 1946. (c) Wasielewski, M. R.; Breslow, R. *J. Am. Chem. Soc.* **1976**, *98*, 4222. (d) Arnett, E. M.; Amarnath, K.; Harvey, N. G.; Cheng, J.-P. *J. Am. Chem. Soc.* **1990**, *112*, 344. (e) Patz, M.; Mayr, H.; Maruta, J.; Fukuzumi, S. *Angew. Chem., Int. Ed. Engl.* **1995**, *34*, 1225.

(34) Mann, C. K.; Barnes, K. K. In *Electrochemical Reaction in Nonaqueous Systems*; Marcel Dekker: New York, 1970.

(32) Fukuzumi, S.; Tokuda, Y.; Kitano, T.; Okamoto, T.; Otera, J. *J. Am. Chem. Soc.* **1993**, *115*, 8960.

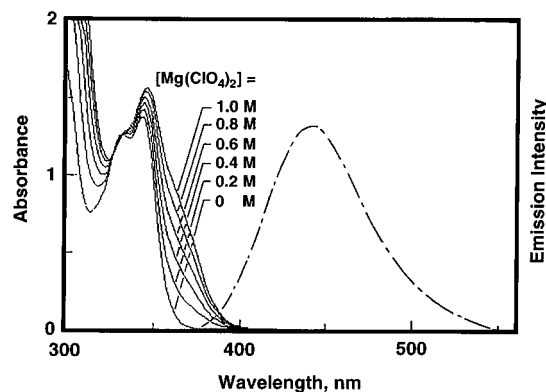


**Figure 1.** Spectral change observed upon addition of  $\text{Mg}(\text{ClO}_4)_2$  to an MeCN solution of 2-naphthaldehyde ( $6.5 \times 10^{-3}$  M) in a 1 mm quartz cell ( $[\text{Mg}(\text{ClO}_4)_2] = 0, 0.20, 0.40, 0.60, 0.80,$  and  $1.0$  M) and the fluorescence spectrum of the  $\text{Mg}(\text{ClO}_4)_2$  complex (broken line) in the presence of  $\text{Mg}(\text{ClO}_4)_2$  (1.0 M) in MeCN at 298 K.

**Table 1.** Formation Constants ( $K$ ), Fluorescence Maxima ( $\lambda_{\text{max}}$ ), Fluorescence Lifetimes ( $\tau$ ), the One-Electron Reduction Potentials ( $E_{\text{red}}^0$ ) of the Singlet Excited States of  $\text{Mg}(\text{ClO}_4)_2$  and  $\text{Sc}(\text{OTf})_3$  Complexes of Aromatic Carbonyl Compounds, and Intrinsic Barriers of Electron Transfer ( $\Delta G_{0,}^{\ddagger}$ )

aromatic carbonyl–metal ion salt complex	$K^a$ $\text{M}^{-1}$	$\lambda_{\text{max}}$ , nm	$\tau$ , ns	$E_{\text{red}}^0$ vs SCE, <sup>b,c</sup> V	$\Delta G_{0,}^{\ddagger}$ , <sup>b</sup> kcal mol <sup>-1</sup>
1-NA– $\text{Mg}(\text{ClO}_4)_2$	0.17	437	6.7	1.97 (0.83)	2.3
1-NA– $\text{Sc}(\text{OTf})_3$	2.8	487	10.0	2.11 (0.83)	2.3
2-NA– $\text{Mg}(\text{ClO}_4)_2$	0.27	440	10.3	1.87 (0.90)	2.3
1-AN– $\text{Mg}(\text{ClO}_4)_2$		432	3.3	1.90 (0.60)	2.7
2-AN– $\text{Mg}(\text{ClO}_4)_2$	0.51	430	11.8	1.77 (0.65)	2.3

<sup>a</sup> Determined from the spectral change of aromatic carbonyl compounds in the presence of  $\text{Mg}(\text{ClO}_4)_2$  and  $\text{Sc}(\text{OTf})_3$ . <sup>b</sup> Determined by adaptation of the free energy relationship for photoinduced electron-transfer reactions (see text). <sup>c</sup> Values in parentheses are those for the triplet excited states of uncomplexed compounds.

All experiments were performed at 298 K. The detailed procedures for the measurements are available in the Supporting Information (S2–S3).

**Phosphorescence Experiments.** The phosphorescence spectra were measured on a Hitachi 850 fluorescence phosphorescence spectrophotometer. Typically, a 2-methyltetrahydrofuran solution (1 mL) containing 1-NA ( $1.5 \times 10^{-3}$  M) in the presence of various concentrations of  $\text{Sc}(\text{OTf})_3$  ( $1.0 \times 10^{-3}$  to  $2.9 \times 10^{-1}$  M) in the capillary cell was degassed by bubbling with argon gas for 15 min. The solution was irradiated with monochromatized light ( $\lambda = 360$  nm) from a xenon lamp and phosphorescence spectra were measured at 77 K. The phosphorescence spectra were measured from 400 to 600 nm.

## Results and Discussion

**Change in Spin State of Photoexcited States by Complexation with Metal Ions.** Addition of  $\text{Mg}(\text{ClO}_4)_2$  to an MeCN solution of 2-naphthaldehyde (2-NA) results in a red shift of ca. 20 nm in the absorption band as shown in Figure 1. The appearance of a new absorption band at 360 nm is ascribed to the 1:1 complex formation between  $\text{Mg}(\text{ClO}_4)_2$  and the carbonyl compound.  $\text{Mg}(\text{ClO}_4)_2$  also forms complexes with other aromatic carbonyl compounds, 2-naphthaldehyde (2-NA), 1-acetonaphthone (1-AN), and 2-acetonaphthone (2-AN). The formation constants ( $K$ ) at 298 K are determined from the spectral changes in the presence of various concentrations of  $\text{Mg}(\text{ClO}_4)_2$  (see Experimental Section), and the  $K$  values are listed in Table 1.

Although aromatic carbonyl compounds are nonfluorescent, irradiation of the new absorption band of 2-NA in the presence of  $\text{Mg}(\text{ClO}_4)_2$  in MeCN causes strong fluorescence at 440 nm

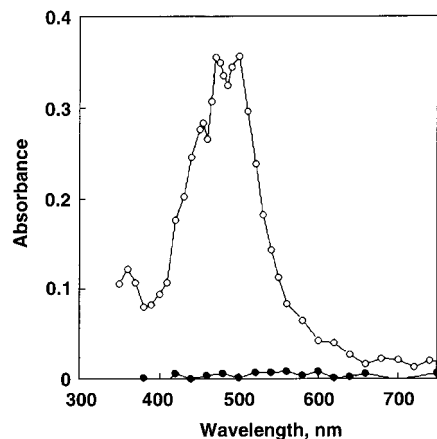


**Figure 2.** T–T absorption spectra by laser-flash photolysis of 1-naphthaldehyde ( $1.0 \times 10^{-3}$  M) in the absence (○) and presence (●) of  $\text{Mg}(\text{ClO}_4)_2$  (1.0 M) in deaerated MeCN at 298 K at  $2.0 \times 10^{-7}$  s after laser irradiation at  $\lambda = 355$  nm.

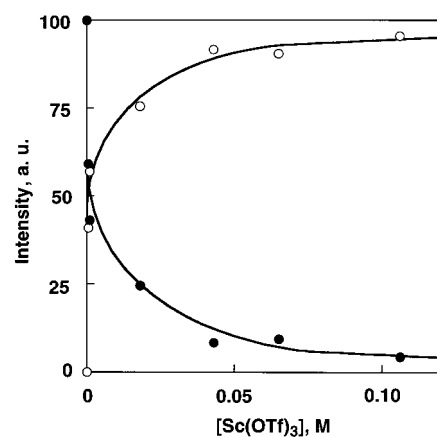


**Figure 3.** Plots of the intensity ratio of fluorescence (○) at  $\lambda_{\text{max}} = 487$  nm at 298 K; phosphorescence (●) at  $\lambda_{\text{max}} = 548$  nm vs  $[\text{Sc}(\text{OTf})_3]$  for 1-naphthaldehyde ( $1.5 \times 10^{-3}$  M) in 2-methyltetrahydrofuran at 77 K.

(Figure 1). When  $\text{Mg}(\text{ClO}_4)_2$  is replaced by  $\text{Sc}(\text{OTf})_3$ , the fluorescence maximum ( $\lambda_{\text{max}}$ ) is red-shifted to 510 nm. Fluorescence is generally observed for other  $\text{Mg}(\text{ClO}_4)_2$ –carbonyl complexes. The fluorescence lifetimes ( $\tau$ ) of the  $\text{Mg}(\text{ClO}_4)_2$ –carbonyl complexes in MeCN at 298 K were determined by single-photon counting (see Experimental Section). The  $\lambda_{\text{max}}$  and  $\tau$  values are also listed in Table 1.

The absence of the triplet excited state for the 1-NA– $\text{Mg}(\text{ClO}_4)_2$  complex is confirmed as the disappearance of the triplet–triplet absorption of 1-NA at 500 nm in the presence of 1.0 M  $\text{Mg}(\text{ClO}_4)_2$  in MeCN (Figure 2). The change in spin state of the lowest excited state from the triplet to the singlet due to the complexation with  $\text{Sc}(\text{OTf})_3$  has also been demonstrated clearly in Figure 3, where the phosphorescence intensity at 548 nm measured at 77 K decreases accompanied by the increased fluorescence intensity at 487 nm measured at 298 K with increasing  $\text{Sc}(\text{OTf})_3$  concentration in 2-methyltetrahydrofuran.

The change in the lowest excited state may be caused by the complexation of aromatic carbonyl compounds with  $\text{Mg}(\text{ClO}_4)_2$ . The nonbonding orbitals are more stabilized by the complex formation with  $\text{Mg}(\text{ClO}_4)_2$  than  $\pi$ -orbitals due to the stronger interaction between nonbonding electrons and  $\text{Mg}(\text{ClO}_4)_2$ . Thus, the  $\pi, \pi^*$  excited state becomes the lowest excited state in the  $\text{Mg}(\text{ClO}_4)_2$  complex as compared with the lowest  $n, \pi^*$  triplet excited state in the uncomplexed carbonyl compound. The

**Table 2.** Fluorescence Quenching Rate Constants ( $k_q$ ) of the  $\text{Mg}(\text{ClO}_4)_2$  and  $\text{Sc}(\text{OTf})_3$  Complexes<sup>a</sup> of Aromatic Carbonyl Compounds by Electron Donors in Deaerated MeCN at 298 K and One-Electron Oxidation Potentials ( $E_{\text{ox}}^0$ ) of the Donors

alkylbenzene	$E_{\text{ox}}^0$ vs SCE, <sup>c</sup> V	$k_q^b$ ( $\text{M}^{-1} \text{s}^{-1}$ ) of the $\text{Mg}(\text{ClO}_4)_2$ complex of			
		1-NA	2-NA	1-AN	2-AN
toluene	2.20	<i>d</i> ( $2.0 \times 10^8$ )	<i>d</i>	<i>d</i>	<i>d</i>
ethylbenzene	2.14	<i>d</i> ( $1.2 \times 10^9$ )	<i>d</i>	<i>d</i>	<i>d</i>
<i>m</i> -xylene	2.02	$6.1 \times 10^8$ ( $3.2 \times 10^9$ )	<i>d</i>	<i>d</i>	<i>d</i>
<i>o</i> -xylene	1.98	( $4.2 \times 10^9$ )	<i>d</i>	<i>d</i>	<i>d</i>
<i>p</i> -cymene	1.96	$2.6 \times 10^9$	$2.7 \times 10^8$	$3.5 \times 10^8$	<i>d</i>
<i>p</i> -xylene	1.93	$3.2 \times 10^9$ ( $5.6 \times 10^9$ )	$4.3 \times 10^8$	$3.5 \times 10^8$	$5.1 \times 10^7$
1,2,3-trimethylbenzene	1.88	$4.0 \times 10^9$	<i>e</i>	<i>e</i>	$8.0 \times 10^7$
1,2,4-trimethylbenzene	1.79	$5.5 \times 10^9$ ( $7.9 \times 10^9$ )	$3.9 \times 10^9$	$3.6 \times 10^9$	$9.9 \times 10^8$
1,2,3,4-tetramethylbenzene	1.71	$6.3 \times 10^9$	$5.3 \times 10^9$	<i>e</i>	$3.8 \times 10^9$
1,2,3,5-tetramethylbenzene	1.71	<i>e</i> ( $8.2 \times 10^9$ )	$5.2 \times 10^9$	$4.6 \times 10^9$	<i>e</i>
pentamethylbenzene	1.58	<i>e</i>	$6.3 \times 10^9$	<i>e</i>	$5.5 \times 10^9$

<sup>a</sup> Values in parentheses are those for the  $\text{Sc}(\text{OTf})_3$  complex;  $[\text{Sc}(\text{OTf})_3] = 1.0 \times 10^{-2} \text{ M}$ . <sup>b</sup> The experimental errors are within  $\pm 10\%$ ;  $[\text{Mg}(\text{ClO}_4)_2] = 1.0 \text{ M}$ . <sup>c</sup> Measured by the second harmonic ac voltammetry using an  $\text{Ag}/\text{AgNO}_3$  (0.01 M) reference electrode and converted to the value vs SCE. All values obtained in deaerated MeCN containing 0.10 M tetrabutylammonium perchlorate at 298 K using a Pt working electrode and a Pt wire auxiliary electrode at a scan rate of  $4 \text{ mV s}^{-1}$ ,  $\Delta E$  (ac amplitude) = 25 mV,  $f$  (ac frequency) = 25 Hz. <sup>d</sup> Too slow to determine accurately. <sup>e</sup> Not determined.

picosecond studies by Boldridge et al.<sup>35</sup> clearly show that the triplet  $\pi, \pi^*$  state of naphthaldehydes is populated through the triplet  $n, \pi^*$  state formed from the first excited singlet  $n, \pi^*$  state by the fast intersystem crossing. Since the singlet–triplet energy gap is substantially larger in the  $\pi, \pi^*$  state than the  $n, \pi^*$  state, the singlet  $\pi, \pi^*$  state being the lowest excited state in the  $\text{Mg}(\text{ClO}_4)_2$  complex becomes strongly fluorescent.

**Change in the Redox Potentials of Photoexcited States by Complexation with Metal Ions.** The free energy change of photoinduced electron transfer from electron donors to the singlet excited states ( $\Delta G_{\text{et}}^0$  in eV) is given by eq 2, where  $e$  is elementary charge,  $E_{\text{ox}}^0$  and  $E_{\text{red}}^*$  are the one-electron oxidation potential of electron donors and the one-electron reduction

$$\Delta G_{\text{et}}^0 = e(E_{\text{ox}}^0 - E_{\text{red}}^*) \quad (2)$$

potentials of the excited states of electron acceptors, respectively. The dependence of the activation free energy change of photoinduced electron transfer ( $\Delta G_{\text{et}}^\ddagger$ ) on  $\Delta G_{\text{et}}^0$  has well been established as given by eq 3,<sup>36</sup> where  $\Delta G_{\text{et}}^{\ddagger 0}$  is the intrinsic barrier that represents the activation free energy change when the

$$\Delta G_{\text{et}}^\ddagger = (\Delta G_{\text{et}}^0/2) + [(\Delta G_{\text{et}}^0/2)^2 + (\Delta G_{\text{et}}^{\ddagger 0})^2]^{1/2} \quad (3)$$

driving force of electron transfer is zero, i.e.,  $\Delta G_{\text{et}}^\ddagger = \Delta G_{\text{et}}^{\ddagger 0}$  at  $\Delta G_{\text{et}}^0 = 0$ . The  $\Delta G_{\text{et}}^\ddagger$  values are obtained from the fluorescence quenching rate constant ( $k_q$ ) by eq 4, where  $Z$  is the collision frequency that is taken as  $1 \times 10^{11} \text{ M}^{-1} \text{ s}^{-1}$ ,  $k_B$  is the Boltzmann constant, and  $k_{\text{diff}}$  is the diffusion rate constant in MeCN.<sup>36</sup>

$$\Delta G_{\text{et}}^\ddagger = (2.3k_B T/e) \log[Z(k_q^{-1} - k_{\text{diff}}^{-1})] \quad (4)$$

The quenching rate constants ( $k_q$ ) of the photoinduced electron transfer from a series of alkylbenzene electron donors to the  $\text{Mg}(\text{ClO}_4)_2$  complexes of naphthaldehydes and acetonaphthones were determined from the fluorescence quenching of the  $\text{Mg}(\text{ClO}_4)_2$ –carbonyl complexes by alkylbenzenes as listed in Table

(35) Boldridge, D. W.; Justus, B. L.; Scott, G. W. *J. Chem. Phys.* **1984**, *80*, 3179.

(36) (a) Rehm, A.; Weller, A. *Ber. Bunsen-Ges. Phys. Chem.* **1969**, *73*, 834. (b) Rehm, A.; Weller, A. *Isr. J. Chem.* **1970**, *8*, 259.

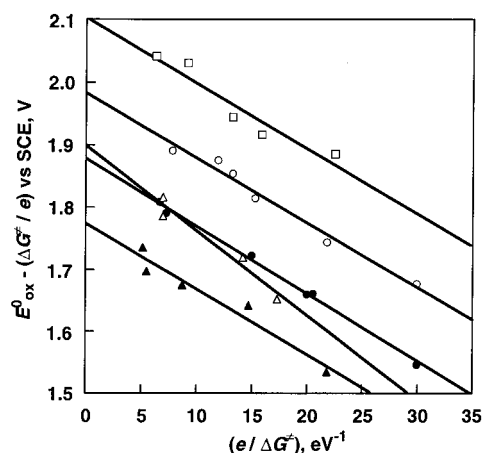


**Figure 4.** Plots of  $E_{\text{ox}}^0 - (\Delta G_{\text{et}}^\ddagger/e)$  vs  $e/\Delta G_{\text{et}}^\ddagger$  for electron transfer from benzene derivatives to the singlet excited states of  $\text{Mg}(\text{ClO}_4)_2$  complexes of 1-naphthaldehyde (○), 2-naphthaldehyde (●), 1-acetonaphthone (Δ), and 2-acetonaphthone (▲), and the singlet excited states of  $\text{Sc}(\text{OTf})_3$  complexes of 1-naphthaldehyde (□); see eq 5 in text.

2 (see Experimental Section). The  $k_q$  value increases with a decrease in the  $E_{\text{ox}}^0$  values of alkyl benzene donors to reach a diffusion-limited value as expected from eqs 2–4 (Table 2). The  $E_{\text{red}}^*$  values (vs SCE) of the singlet excited states of the  $\text{Mg}^{2+}$ –carbonyl complexes can be determined from the dependence of  $k_q$  on  $E_{\text{ox}}^0$  as follows. From eqs 2–4 is derived a linear relation between  $E_{\text{ox}}^0 - (\Delta G_{\text{et}}^\ddagger/e)$  and  $(\Delta G_{\text{et}}^\ddagger/e)^{-1}$  as given by eq 5. Thus, the unknown values of  $E_{\text{red}}^*$  and  $\Delta G_{\text{et}}^{\ddagger 0}$  can be determined from the intercept and slope of the linear plots of

$$E_{\text{ox}}^0 - (\Delta G_{\text{et}}^\ddagger/e) = E_{\text{red}}^* - (\Delta G_{\text{et}}^{\ddagger 0}/e)^2/(\Delta G_{\text{et}}^\ddagger/e) \quad (5)$$

$E_{\text{ox}}^0 - (\Delta G_{\text{et}}^\ddagger/e)$  vs  $(\Delta G_{\text{et}}^\ddagger/e)^{-1}$  as shown in Figure 4.<sup>37</sup> The  $E_{\text{red}}^*$  and  $\Delta G_{\text{et}}^{\ddagger 0}$  values of the  $\text{Mg}(\text{ClO}_4)_2$ –carbonyl complexes thus obtained are listed in Table 1. The  $E_{\text{red}}^0$  values of ground states of the carbonyl compounds were determined by the cyclic voltammograms and the second-harmonic alternating current

(37) The  $k_{\text{diff}}$  value is taken as  $8.2 \times 10^9 \text{ M}^{-1} \text{ s}^{-1}$ , which is the maximum value in Table 2.

voltammograms (see Experimental Section).<sup>33</sup> The  $E_{\text{red}}^0$  values of the triplet excited states are obtained by adding the triplet excitation energies<sup>38</sup> as also listed in Table 1. The comparison of the  $E_{\text{red}}^0$  values between the triplet excited states of uncomplexed carbonyl compounds and the singlet excited states of the  $\text{Mg}(\text{ClO}_4)_2$  complexes in Table 1 reveals the remarkable positive shifts (ca. 1.2 V) of the  $E_{\text{red}}^0$  values of the singlet excited states of the  $\text{Mg}(\text{ClO}_4)_2$ -carbonyl complexes as compared to those of the triplet excited states of uncomplexed carbonyl compounds. Such large positive shifts of the  $E_{\text{red}}^0$  values result in a significant increase in the reactivity of the  $\text{Mg}(\text{ClO}_4)_2$  complexes vs uncomplexed carbonyl compounds in the photoinduced electron-transfer reactions as shown in Table 2.

The promoting effect of  $\text{Mg}(\text{ClO}_4)_2$  on the photoinduced electron-transfer reactions of aromatic carbonyl compounds is certainly related to the Lewis acidity of the metal ion salt. We have recently reported that the  $g_{zz}$ -values of ESR spectra of superoxide-metal ion complexes are highly sensitive to the Lewis acidity of a variety of metal ions and that the binding energies ( $\Delta E$ ) readily derived from the  $g_{zz}$ -values provide the quantitative experimental measure of Lewis acidity of a wide variety of metal ions.<sup>39</sup> The  $\Delta E$  values have been shown to be directly correlated with the promoting effects of metal ion salts in electron-transfer reactions.<sup>39</sup> It has been found that  $\text{Sc}(\text{OTf})_3$  is the strongest Lewis acid among monovalent, divalent, and trivalent metal ion salts.<sup>39</sup> Thus, the rate constants of the photoinduced electron transfer from a series of alkylbenzene electron donors to the  $\text{Sc}(\text{OTf})_3$  complex of 1-NA were also determined from the fluorescence quenching of the  $\text{Sc}(\text{OTf})_3$  complex of 1-NA by alkylbenzenes as listed in Table 2. Although no quenching of the fluorescence of an  $\text{Mg}(\text{ClO}_4)_2$  complex of 1-NA occurs with toluene, which is the weakest electron donor among alkylbenzene donors employed in this study, the fluorescence of the  $\text{Sc}(\text{OTf})_3$  complex of 1-NA is efficiently quenched by toluene (Table 2). The  $E_{\text{red}}^0$  and  $\Delta G_{\text{red}}^{\ddagger}$  values of the singlet excited state of the 1-NA- $\text{Sc}(\text{OTf})_3$  complex are also determined from the intercept and slope of the linear plots of  $E_{\text{ox}}^0 - (\Delta G_{\text{et}}^{\ddagger}/e)$  vs  $(\Delta G_{\text{et}}^{\ddagger}/e)^{-1}$  (Figure 4). The comparison of the  $E_{\text{red}}^0$  values in Table 1 reveals the further positive shift (0.14 V) of the  $E_{\text{red}}^0$  value of the singlet excited states of the 1-NA- $\text{Sc}(\text{OTf})_3$  complex as compared with the value of the singlet excited state to the 1-NA- $\text{Mg}(\text{ClO}_4)_2$  complex. The overall positive shift from the value of the triplet excited state of 1-NA is as large as 1.3 V, which corresponds to  $10^{22}$  times acceleration in terms of the rate constant of photoinduced electron transfer in the endergonic region ( $\Delta G_{\text{et}}^0 > 0$ ).<sup>40</sup>

In contrast to the case of naphthaldehydes and acetophenones, irradiation of the absorption band of 10-methylacridone (AcrCO) results in fluorescence at 413 nm in MeCN. Thus, AcrCO is chosen as an aromatic carbonyl compound to examine the change in the redox potentials of the singlet excited state by complexation with Lewis acids. When  $\text{Sc}(\text{OTf})_3$  is added to an MeCN solution of AcrCO, the absorption bands of 10-methylacridone are red-shifted due to the 1:1 complex formation between AcrCO and  $\text{Sc}(\text{OTf})_3$  (see Supporting Information, S4). The formation constant ( $K$ ) is determined from the spectral change as  $1.2 \times 10^5 \text{ M}^{-1}$  (see Experimental Section). Thus, the Lewis acidity of  $\text{Sc}(\text{OTf})_3$  is strong enough to form the

**Table 3.** Fluorescence Lifetime ( $\tau$ ) and Emission Maxima ( $\lambda_{\text{max}}$ ) of AcrCO, AcrCO-M(OTf)<sub>3</sub> (M = Mg, La, Lu, and Sc) in MeCN, and AcrCO-Me<sub>3</sub>SiOTf in CH<sub>2</sub>Cl<sub>2</sub> and Lewis Acidity of Metal Ion Salts ( $\Delta E$ )<sup>a</sup>

Lewis acid	$\Delta E$ , eV	$\tau$ , ns	$\lambda_{\text{max}}$ , nm
	0	6.1	413
Mg(OTf) <sub>2</sub>	0.33	12.8	430
La(OTf) <sub>3</sub>	0.50	14.4	446
Lu(OTf) <sub>3</sub>	0.51	15.2	461
Sc(OTf) <sub>3</sub>	0.68	16.9	474
Me <sub>3</sub> SiOTf		20.3	474

<sup>a</sup> Derived from the  $g_{zz}$ -values of ESR spectra of superoxide-metal ion salt complexes as the quantitative measure of the Lewis acidity.<sup>39</sup>

complex with AcrCO in competition with the coordination of MeCN which is an abundant weak base. When AcrCO forms the complex with  $\text{Sc}(\text{OTf})_3$ , the fluorescence maximum is also red-shifted from 413 to 474 nm and the fluorescence lifetime becomes longer in the AcrCO- $\text{Sc}(\text{OTf})_3$  complex (16.9 ns for the <sup>1</sup>AcrCO\*- $\text{Sc}(\text{OTf})_3$  complex and 6.1 ns for <sup>1</sup>AcrCO\*, see Supporting Information, S5). Similarly the fluorescence maxima ( $\lambda_{\text{max}}$ ) and the lifetimes ( $\tau$ ) are changed when AcrCO forms the complexes with various Lewis acids ( $\text{Mg}(\text{ClO}_4)_2$ ,  $\text{La}(\text{OTf})_3$ ,  $\text{Lu}(\text{OTf})_3$ , and  $\text{Me}_3\text{SiOTf}$ ). The results are summarized in Table 3, where the binding energies ( $\Delta E$ ) derived from the  $g_{zz}$ -values of ESR spectra of superoxide-metal ion complexes are given as the quantitative measure of Lewis acidity of the metal ion.<sup>39</sup> The stronger the Lewis acidity of metal ions, the more red-shifted is the  $\lambda_{\text{max}}$  value, and the longer is the excited-state lifetime ( $\tau$ ). The AcrCO- $\text{Sc}(\text{OTf})_3$  complex in MeCN and the AcrCO-Me<sub>3</sub>SiOTf complex in CH<sub>2</sub>Cl<sub>2</sub> have the longest  $\lambda_{\text{max}}$  value. Thus, we have examined the change in the redox potentials of the singlet excited state of AcrCO by complexation with  $\text{Sc}(\text{OTf})_3$  in MeCN and Me<sub>3</sub>SiOTf in CH<sub>2</sub>Cl<sub>2</sub> (vide infra).

The fluorescence quenching rate constants ( $k_q$ ) of the photoinduced electron transfer from a series of electron donors to the AcrCO- $\text{Sc}(\text{OTf})_3$  complex in MeCN and the AcrCO-Me<sub>3</sub>SiOTf complex in CH<sub>2</sub>Cl<sub>2</sub> were determined from the fluorescence quenching by the donors (see Experimental Section). The  $k_q$  values are constant independent of  $[\text{Sc}(\text{OTf})_3]$  or  $[\text{Me}_3\text{SiOTf}]$  in the concentration region where all AcrCO molecules form the complex. The  $k_q$  values are summarized in Table 4, together with the  $E_{\text{ox}}^0$  values of donors in MeCN and CH<sub>2</sub>Cl<sub>2</sub>.

Plots of  $\log k_q$  vs  $E_{\text{ox}}^0$  for the AcrCO- $\text{Sc}(\text{OTf})_3$  complex in MeCN and the AcrCO-Me<sub>3</sub>SiOTf complex in CH<sub>2</sub>Cl<sub>2</sub> are shown in Figure 5. In each case, the  $k_q$  value increases with decreasing the  $E_{\text{ox}}^0$  value to reach a diffusion-limited value. The plots of Figure 5 are fitted using eqs 2-4 as shown by the solid lines, which agree with the experimental results. The best fit lines shown in Figure 5 give the  $E_{\text{red}}^0$  values (1.64 and 1.89 V vs SCE) and  $\Delta G_{\text{red}}^{\ddagger}$  value (2.6 and 2.6 kcal mol<sup>-1</sup>) for the  $\text{Sc}(\text{OTf})_3$ -AcrCO complex in MeCN and the AcrCO-Me<sub>3</sub>SiOTf complex in CH<sub>2</sub>Cl<sub>2</sub>, respectively. As compared to the  $E_{\text{red}}^0$  value of <sup>1</sup>AcrCO\* (1.13 V), the  $E_{\text{red}}^0$  value of the <sup>1</sup>AcrCO\*- $\text{Sc}(\text{OTf})_3$  complex is significantly shifted to the positive direction (0.51 V). The  $E_{\text{red}}^0$  value of the Me<sub>3</sub>SiOTf-AcrCO complex in CH<sub>2</sub>Cl<sub>2</sub> is further shifted (0.76 V). This indicates that Me<sub>3</sub>SiOTf acts as a stronger Lewis acid than  $\text{Sc}(\text{OTf})_3$ .

The large positive shift in the one-electron reduction potential of AcrCO- $\text{Sc}(\text{OTf})_3$  in MeCN is also observed in the ground state as indicated by the electrochemical study. Figure 6 shows the second harmonic ac voltammograms (SHACV)<sup>33</sup> of AcrCO in the absence and presence of  $\text{Sc}(\text{OTf})_3$ . The  $E_{\text{red}}^0$  value of AcrCO (-1.92 V) is shifted to -1.21 V when AcrCO forms the complex with  $\text{Sc}(\text{OTf})_3$ . The zero-zero excitation energy

(38) Herkstroeter, W. G.; Lamola, A. A.; Hammond, G. S. *J. Am. Chem. Soc.* **1964**, *86*, 4537.

(39) Fukuzumi, S.; Ohkubo, K. *Chem. Eur. J.* **2000**, *6*, 4532.

(40) The difference in the  $\log k_{\text{et}}$  value is given by the following equation:  $\Delta \log k_{\text{et}} = -\Delta \Delta G_{\text{et}}^{\ddagger} / (2.3k_{\text{B}}T) = 22$  (at 298 K).

**Table 4.** Oxidation Potentials ( $E_{\text{ox}}^0$ ) of Electron Donors and Fluorescence Quenching Rate Constants ( $k_q$ ) of the AcrCO–Sc(OTf)<sub>3</sub> Complex ( $5.0 \times 10^{-5}$  M) and the AcrCO–Me<sub>3</sub>SiOTf Complex by Electron Donors in MeCN and in CH<sub>2</sub>Cl<sub>2</sub> at 298 K, Respectively

no.	donor	$E_{\text{ox}}^0$ vs SCE, <sup>a</sup> V	$k_q$ , <sup>b</sup> M <sup>-1</sup> s <sup>-1</sup>
1	10-methyl-9,10-dihydroacridine	0.80 (0.90)	$1.6 \times 10^{10}$ ( $1.5 \times 10^{10}$ )
2	9,10-dimethylanthracene	1.05	$1.4 \times 10^{10}$
3	anthracene	1.19	$1.3 \times 10^{10}$
4	hexamethylbenzene	1.49 (1.60)	$5.8 \times 10^9$ ( $8.2 \times 10^9$ )
5	pentamethylbenzene	1.58 (1.68)	$4.2 \times 10^9$ ( $7.6 \times 10^9$ )
6	1,2,4,5-tetramethylbenzene	1.63 (1.75)	$1.4 \times 10^9$ ( $6.6 \times 10^9$ )
7	1,2,3,5-tetramethylbenzene	1.71 (1.77)	$3.8 \times 10^8$ ( $4.7 \times 10^9$ )
8	1,2,3,4-tetramethylbenzene	(1.81)	( $4.4 \times 10^9$ )
9	1,2,4-trimethylbenzene	1.79 (1.89)	$2.8 \times 10^7$ ( $8.2 \times 10^8$ )
10	1,2,3-trimethylbenzene	(1.98)	( $9.1 \times 10^7$ )

<sup>a</sup> Values in parentheses are determined in CH<sub>2</sub>Cl<sub>2</sub>. <sup>b</sup> Values in parentheses are those for the AcrCO–Me<sub>3</sub>SiOTf complex in CH<sub>2</sub>Cl<sub>2</sub>.

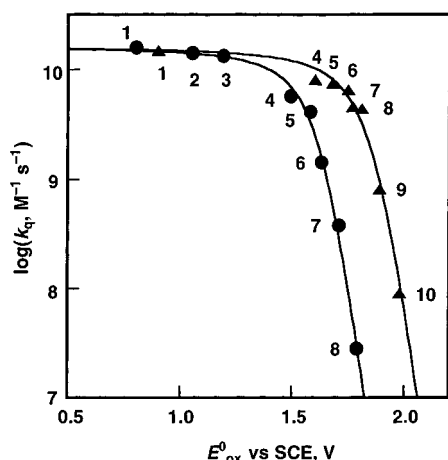


**Figure 5.** Plots of  $\log k_q$  vs  $E_{\text{ox}}^0$  for the fluorescence quenching of AcrCO ( $5.0 \times 10^{-5}$  M) by various electron donors in the presence of Sc(OTf)<sub>3</sub> ( $4.0 \times 10^{-2}$  M) in deaerated MeCN (●) and in the presence of Me<sub>3</sub>SiOTf ( $2.0 \times 10^{-3}$  M) in deaerated dry CH<sub>2</sub>Cl<sub>2</sub> (▲) at 298 K. The numbers refer to compounds in Table 4. The solid lines are drawn based on eqs 2–4.

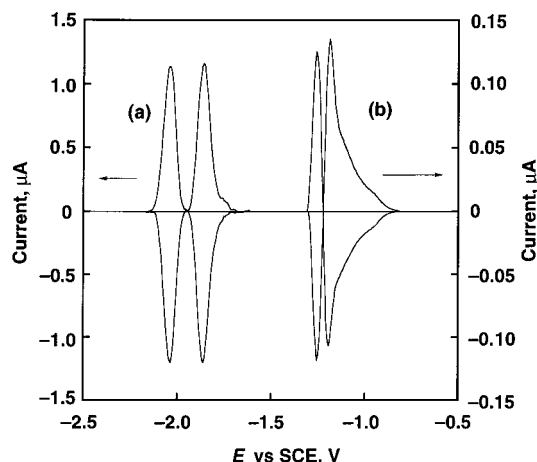


**Figure 6.** SHACVs of (a) AcrCO ( $5.0 \times 10^{-3}$  M) in deaerated MeCN and (b) AcrCO in the presence of Sc(OTf)<sub>3</sub> ( $5.0 \times 10^{-2}$  M) in deaerated EtCN, 0.10 M TBAPF<sub>6</sub> at 298 K. Scan rate = 4 mV s<sup>-1</sup>.

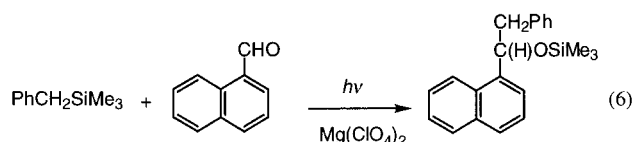
of <sup>1</sup>AcrCO\*–Sc(OTf)<sub>3</sub> ( $\Delta E_{0,0}$ ) can be obtained as 2.81 V from the absorption maximum (413 nm, 3.00 eV) and the fluorescence maximum (474 nm, 2.62 eV). Then, the  $E_{\text{red}}^0$  value of <sup>1</sup>AcrCO\*–Sc(OTf)<sub>3</sub> is determined as 1.60 eV by subtracting the  $\Delta E_{0,0}$  value from the  $E_{\text{red}}^0$  value of the ground-state complex. This value agrees with the value (1.64 V) evaluated from the fluorescence quenching in Figure 5. Similarly, the  $E_{\text{red}}^0$  value of <sup>1</sup>AcrCO\*–Me<sub>3</sub>SiOTf is determined as 1.91 eV, which also

agrees with the value (1.88 V) evaluated from the fluorescence quenching in Figure 5.

**Lewis Acid-Catalyzed Photoaddition of Benzyltrimethylsilane via Photoinduced Electron Transfer.** Since the  $E_{\text{red}}^0$  values of the singlet excited states of naphthaldehyde– and acetonaphthone–Mg(ClO<sub>4</sub>)<sub>2</sub> complexes (Table 1) become higher than the  $E_{\text{ox}}^0$  values of PhCH<sub>2</sub>SiMe<sub>3</sub> (1.38 V),<sup>9a</sup> the photoinduced electron transfer from PhCH<sub>2</sub>SiMe<sub>3</sub> to the singlet excited states of Mg(ClO<sub>4</sub>)<sub>2</sub>–carbonyl complexes would occur efficiently. In fact, the fluorescence of Mg(ClO<sub>4</sub>)<sub>2</sub>–carbonyl complexes is quenched efficiently by PhCH<sub>2</sub>SiMe<sub>3</sub> in MeCN at 298 K. The quenching rate constants ( $k_q$ ) were determined from the fluorescence quenching as listed in Table 5 (see Supporting Information, S6).

The  $\Delta G_{\text{et}}^{\ddagger}$  values of photoinduced electron transfer from PhCH<sub>2</sub>SiMe<sub>3</sub> to the singlet excited states can be evaluated by using eqs 2–4, since the  $\Delta G_{\text{et}}^{\ddagger}$  value for the photoinduced electron transfer of organosilanes such as PhCH<sub>2</sub>SiMe<sub>3</sub> has previously been determined as 4.6 kcal mol<sup>-1</sup>.<sup>9a</sup> The  $k_{\text{et}}$  values which correspond to the  $k_q$  values in eq 4 are calculated as listed in Table 5, where the  $k_{\text{et}}$  values indeed agree with the  $k_q$  values. Such an agreement indicates that the fluorescence quenching of the Mg(ClO<sub>4</sub>)<sub>2</sub>–carbonyl complexes by PhCH<sub>2</sub>SiMe<sub>3</sub> occurs via electron transfer from PhCH<sub>2</sub>SiMe<sub>3</sub> to the singlet excited states of the Mg(ClO<sub>4</sub>)<sub>2</sub>–carbonyl complexes.

No photochemical reaction of naphthaldehydes or acetonaphthones with PhCH<sub>2</sub>SiMe<sub>3</sub> has occurred, as expected from the higher  $E_{\text{ox}}^0$  value of PhCH<sub>2</sub>SiMe<sub>3</sub><sup>9a</sup> than the  $E_{\text{red}}^0$  values of the triplet excited states in Table 1. In the presence of Mg(ClO<sub>4</sub>)<sub>2</sub> (0.94 M), however, irradiation of a deaerated MeCN solution containing PhCH<sub>2</sub>SiMe<sub>3</sub> ( $1.7 \times 10^{-1}$  M) and 1-NA ( $1.4 \times 10^{-3}$  M) with monochromatized light of  $\lambda = 350$  nm results in the decrease in the absorbance due to 1-NA, accompanied by the increase in the absorbance due to the photoproduct with a clean isosbestic point at  $\lambda = 282$  nm (see Supporting Information, S7). The photoproduct is identified as the benzyl adduct as shown in eq 6 (see Experimental Section).<sup>24,41,42</sup> The benzyl adducts are also obtained in the photochemical reactions of other carbonyl compounds (2-NA, 1-AN, 2-AN) with PhCH<sub>2</sub>SiMe<sub>3</sub> in the presence of Mg(ClO<sub>4</sub>)<sub>2</sub> in MeCN (see Experimental Section).

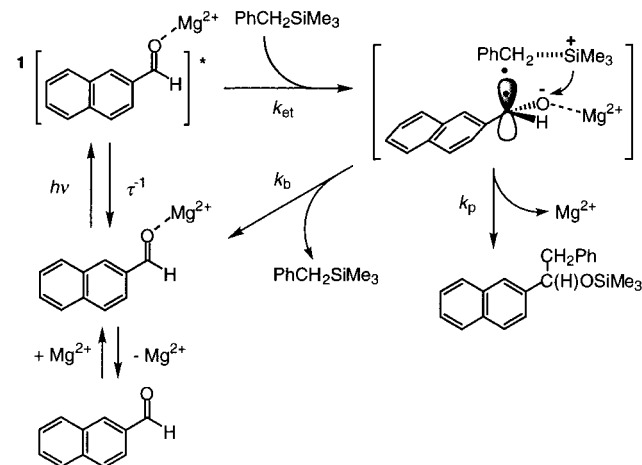


The quantum yields ( $\Phi$ ) of the photoaddition reactions in the presence of Mg(ClO<sub>4</sub>)<sub>2</sub> (1.0 M) increase with an increase in [PhCH<sub>2</sub>SiMe<sub>3</sub>] to reach a constant value ( $\Phi_{\infty}$ ) (see Supporting

**Table 5.** Fluorescence Quenching Rate Constants ( $k_q$ ), Rate Constants ( $k_{et}$ ) of Photoinduced Electron Transfer from  $\text{PhCH}_2\text{SiMe}_3$  and  $\text{Me}_4\text{Sn}$  to the Singlet Excited States of  $\text{Mg}(\text{ClO}_4)_2^-$  and  $\text{Sc}(\text{OTf})_3^-$ -Carbonyl Complexes, and Observed Rate Constants ( $k_{obs}$ ) and Limiting Quantum Yields ( $\Phi_\infty$ ) for Photoaddition of  $\text{PhCH}_2\text{SiMe}_3$  and  $\text{Me}_4\text{Sn}$  with  $\text{Mg}(\text{ClO}_4)_2^-$  and  $\text{Sc}(\text{OTf})_3^-$ -Carbonyl Complexes in Deaerated MeCN at 298 K

reactant pair compd	$k_q^a$ , $\text{M}^{-1} \text{s}^{-1}$	$k_{et}^b$ , $\text{M}^{-1} \text{s}^{-1}$	$k_{obs}^c$ , $\text{M}^{-1} \text{s}^{-1}$	$\Phi_\infty^c$
$\text{PhCH}_2\text{SiMe}_3/1\text{-NA-Mg}(\text{ClO}_4)_2$	$4.9 \times 10^9$	$4.3 \times 10^9$	$5.4 \times 10^9$	$9.6 \times 10^{-2}$
$\text{PhCH}_2\text{SiMe}_3/2\text{-NA-Mg}(\text{ClO}_4)_2$	$4.3 \times 10^9$	$3.6 \times 10^9$	$4.6 \times 10^9$	$7.1 \times 10^{-2}$
$\text{PhCH}_2\text{SiMe}_3/1\text{-AN-Mg}(\text{ClO}_4)_2$	$3.7 \times 10^9$	$3.8 \times 10^9$	$3.9 \times 10^9$	$1.0 \times 10^{-1}$
$\text{PhCH}_2\text{SiMe}_3/2\text{-AN-Mg}(\text{ClO}_4)_2$	$3.0 \times 10^9$	$2.6 \times 10^9$	$3.5 \times 10^9$	$1.1 \times 10^{-1}$
$\text{Me}_4\text{Sn}/1\text{-NA-Sc}(\text{OTf})_3$	$1.8 \times 10^8$	$1.6 \times 10^7$ ( $1.0 \times 10^8$ )	$1.5 \times 10^8$	$3.3 \times 10^{-1}$
$\text{PhCH}_2\text{SiMe}_3/\text{AcrCO-Sc}(\text{OTf})_3$	$7.9 \times 10^8$	$9.6 \times 10^8$	$8.9 \times 10^8$	$3.9 \times 10^{-2}$

<sup>a</sup> Determined from Stern–Volmer plots for the fluorescence quenching (eq 1, see Supporting Information, S6). <sup>b</sup> Calculated based on the free energy relationship for the photoinduced electron transfer using eqs 2–4. The value in parentheses is that calculated based on the Marcus equation (eq 10, see text). <sup>c</sup> Determined from the dependence of  $\Phi$  on the substrate concentration.

**Scheme 1**

Information, S8) in accordance with eq 7. From the linear plots of  $\Phi^{-1}$  vs  $[\text{PhCH}_2\text{SiMe}_3]^{-1}$  are obtained the values of  $\Phi_\infty$  and

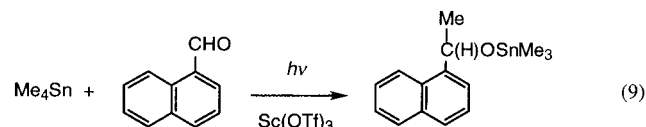
$$\Phi = \Phi_\infty k_{obs} \tau [\text{PhCH}_2\text{SiMe}_3] / (1 + k_{obs} \tau [\text{PhCH}_2\text{SiMe}_3]) \quad (7)$$

the rate constants ( $k_{obs}$ ), which are also listed in Table 5. The  $k_{obs}$  values agree well with both the  $k_q$  and  $k_{et}$  values. Such an agreement strongly indicates that the photoaddition reactions proceed via photoinduced electron transfer from  $\text{PhCH}_2\text{SiMe}_3$  to the singlet excited states of the  $\text{Mg}(\text{ClO}_4)_2^-$ -carbonyl complexes ( $k_{et}$ ), followed by the cleavage of the Si–C bond in the radical cation<sup>43,44</sup> and the radical coupling with the carbonyl radical anion ( $k_p$ ) to yield the adduct in competition with the back electron transfer to the reactant pair ( $k_b$ ) as shown in Scheme 1 for the case of the  $\text{PhCH}_2\text{SiMe}_3/2\text{-NA-Mg}(\text{ClO}_4)_2$  system.<sup>45,46</sup> The rapid cleavage of the Si–C bond in the radical cation<sup>43,44</sup> is consistent with relatively large quantum yields (Table 5) which are higher than one would normally expect for singlet radical ion chemistry for which energy wasting back electron transfer usually dominates.<sup>47</sup>

By application of the steady-state approximation to the reactive species in Scheme 1, the dependence of  $\Phi$  on  $[\text{PhCH}_2\text{SiMe}_3]$  can be derived as given by eq 8, which agrees with the observed dependence of  $\Phi$  on  $[\text{PhCH}_2\text{SiMe}_3]$  (eq 7). The observed rate constant ( $k_{obs}$ ) and the limiting quantum yield ( $\Phi_\infty$ ) correspond to the rate constant ( $k_{et}$ ) of photoinduced electron transfer from  $\text{PhCH}_2\text{SiMe}_3$  to the  $\text{Mg}(\text{ClO}_4)_2^-$ -carbonyl complexes and  $k_p/(k_p + k_b)$ , respectively.

$\Phi = [k_p/(k_p + k_b)]k_{et}\tau[\text{PhCH}_2\text{SiMe}_3]/(1 + k_{et}\tau[\text{PhCH}_2\text{SiMe}_3]) \quad (8)$

When  $\text{PhCH}_2\text{SiMe}_3$  is replaced by a much weaker electron donor such as tetramethyltin ( $\text{Me}_4\text{Sn}$ ), no photoaddition of  $\text{Me}_4\text{Sn}$  with the 1-NA- $\text{Mg}(\text{ClO}_4)_2$  complex has occurred. In the case of the 1-NA- $\text{Sc}(\text{OTf})_3$  complex, however, the photoaddition of  $\text{Me}_4\text{Sn}$  occurs efficiently to yield the methyl adduct (see Experimental Section and eq 9).



It has been reported that no photoinduced electron transfer from  $\text{Me}_4\text{Sn}$  to the singlet excited state of a flavin analogue ( $E_{red}^0 = 1.96 \text{ V}$ ) occurs.<sup>48</sup> Since this  $E_{red}^0$  value is nearly the same as the value of the singlet excited state of the 1-NA- $\text{Mg}(\text{ClO}_4)_2^-$  complex ( $E_{red}^0 = 1.98 \text{ V}$ ), no photoinduced electron transfer from  $\text{Me}_4\text{Sn}$  to the singlet excited state of the 1-NA- $\text{Mg}(\text{ClO}_4)_2^-$  complex would occur. In fact, no fluorescence quenching of the 1-NA- $\text{Mg}(\text{ClO}_4)_2^-$  complex has occurred by  $\text{Me}_4\text{Sn}$ . In contrast to the  $\text{Mg}(\text{ClO}_4)_2^-$  complex, the fluorescence of the 1-NA- $\text{Sc}(\text{OTf})_3^-$  complex is quenched efficiently by  $\text{Me}_4\text{Sn}$ . The quenching rate constant  $k_q$  was determined from the fluorescence quenching as listed in Table 5.

(41) In this case, no homo-coupling products such as dibenzyl have been detected (see Experimental Section) in contrast with the case of the photoalkylation of 10-methylacridinium ion by a bulky electron donor such as diphenylmethane via photoinduced electron transfer in which the hetero-coupling between diphenylmethyl radical and acridinyl radical is retarded due to the steric effects to yield the homo-coupling product (13% yield).<sup>42</sup>

(42) Fujita, M.; Ishida, A.; Takamuku, S.; Fukuzumi, S. *J. Am. Chem. Soc.* **1996**, *118*, 8566.

(43) (a) Dinnocenzo, J. P.; Farid, S.; Goodman, J. L.; Gould, I. R.; Todd, W. P.; Mattes, S. L. *J. Am. Chem. Soc.* **1989**, *111*, 8973. (b) Cermenati, L.; Freccero, M.; Venturello, P.; Albini, A. *J. Am. Chem. Soc.* **1995**, *117*, 7869.

(44) Dockery, K. P.; Dinnocenzo, J. P.; Farid, S.; Goodman, J. L.; Gould, I. R.; Todd, W. P. *J. Am. Chem. Soc.* **1997**, *119*, 1876.

(46) (a) Barton, D. H. R.; Dalko, P. I.; Géro, S. D. *Tetrahedron Lett.* **1992**, *33*, 1883. (b) Barton, D. H. R.; Haynes, R. K.; Leclerc, G.; Magnus, P. D.; Menzies, I. D. *J. Chem. Soc., Perkin Trans. 1* **1975**, 2055. (c) Barton, D. H. R.; Haynes, R. K.; Magnus, P. D.; Menzies, I. D. *J. Chem. Soc., Chem. Commun.* **1974**, 511.

(47) A referee suggested to add this discussion.

(48) Fukuzumi, S.; Kuroda, S.; Tanaka, T. *J. Chem. Soc., Perkin Trans. 2* **1986**, 25.

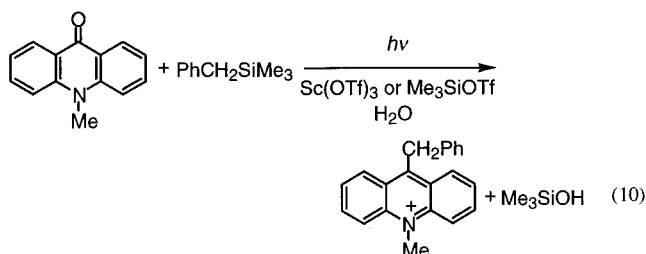


The  $k_{\text{obs}}$  and  $\Phi_{\infty}$  values were also determined from the dependence of  $\Phi$  on  $[\text{Me}_4\text{Sn}]$  (see Supporting Information, S9) as listed in Table 5, where the  $k_{\text{obs}}$  value agrees with the  $k_{\text{q}}$  value. The rate constant ( $k_{\text{et}}$ ) of photoinduced electron transfer from  $\text{Me}_4\text{Sn}$  to the singlet excited state of the 1-NA- $\text{Sc}(\text{OTf})_3$  complex can be evaluated by using eqs 2–4, since the  $\Delta G^{\ddagger}_0$  value for the electron transfer of  $\text{Me}_4\text{Sn}$  has previously been determined as  $10.2 \text{ kcal mol}^{-1}$ .<sup>48–50</sup> The  $k_{\text{et}}$  value thus evaluated is also listed in Table 5, where the  $k_{\text{et}}$  value ( $1.6 \times 10^7 \text{ M}^{-1} \text{ s}^{-1}$ ) is smaller than the  $k_{\text{q}}$  and  $k_{\text{obs}}$  values. When the  $\Delta G^{\ddagger}_0$  value is large, the Marcus equation (eq 10)<sup>51</sup> is known to fit better with the experimental results than the Rehm–Weller equation (eq 3).<sup>48–52</sup>

$$\Delta G^{\ddagger}_{\text{et}} = \Delta G^{\ddagger}_0 [1 + (\Delta G^0_{\text{et}}/4\Delta G^{\ddagger}_0)^2] \quad (10)$$

The calculated  $k_{\text{et}}$  value ( $1.0 \times 10^8 \text{ M}^{-1} \text{ s}^{-1}$ ) using eq 10 instead of eq 3 is given in parenthesis in Table 5. This value agrees with the experimental values ( $k_{\text{q}}$  and  $k_{\text{obs}}$ ).<sup>53</sup> Such an agreement indicates that the photoaddition reaction proceeds via photoinduced electron transfer from  $\text{Me}_4\text{Sn}$  to the singlet excited state of the 1-NA- $\text{Sc}(\text{OTf})_3$  complex, followed by the cleavage of the Sn–C bond in the radical cation and the radical coupling with the carbonyl radical anion as is the case for the photoaddition of  $\text{PhCH}_2\text{SiMe}_3$  in Scheme 1.

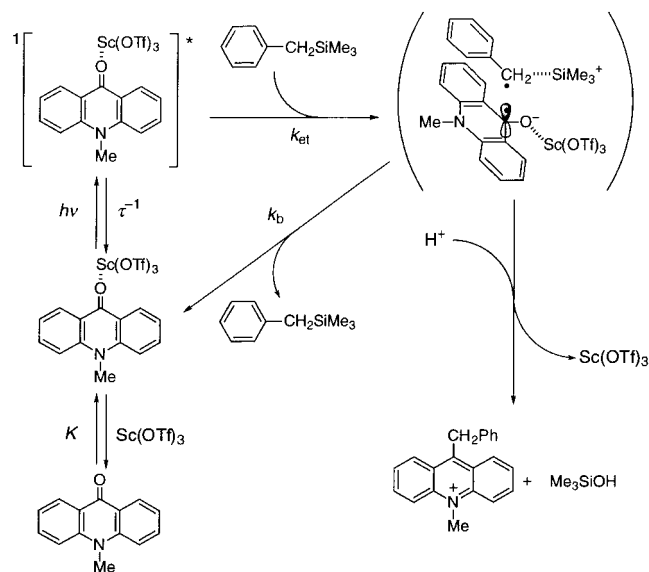
Photoaddition of  $\text{PhCH}_2\text{SiMe}_3$  with  $\text{AcrCO}$  is also made possible when  $\text{AcrCO}$  forms the complex with  $\text{Sc}(\text{OTf})_3$  and  $\text{Me}_3\text{SiOTf}$  (vide infra). The photoirradiation of the absorption band of the  $\text{AcrCO-Sc}(\text{OTf})_3$  complex in the presence of  $\text{PhCH}_2\text{SiMe}_3$  with monochromatized visible light ( $\lambda = 413 \text{ nm}$ ) results in an efficient photochemical reaction of the  $\text{AcrCO-Sc}(\text{OTf})_3$  complex with  $\text{PhCH}_2\text{SiMe}_3$  to yield 9-benzyl-10-methylacridinium ion as shown in eq 10 (see Experimental



Section). Essentially the same results were obtained when the photochemical reaction was performed in the presence of  $\text{Me}_3\text{SiOTf}$  in dry  $\text{CH}_2\text{Cl}_2$  instead of  $\text{Sc}(\text{OTf})_3$  in  $\text{MeCN}$ .

As is the case of  $\text{Mg}(\text{ClO}_4)_2$ - and  $\text{Sc}(\text{OTf})_3$ -catalyzed photoaddition reactions of  $\text{PhCH}_2\text{SiMe}_3$  and  $\text{Me}_4\text{Sn}$  described above, the  $k_{\text{q}}$ ,  $k_{\text{obs}}$ , and  $\Phi_{\infty}$  values are determined as listed in Table 5 (see Supporting Information, S10). The rate constants ( $k_{\text{et}}$ ) of photoinduced electron transfer from  $\text{PhCH}_2\text{SiMe}_3$  to the singlet excited state complex [ $^1\text{AcrCO}^*-\text{Sc}(\text{OTf})_3$ ] can be evaluated by using eqs 2–4 and the  $\Delta G^{\ddagger}_0$  value for the photoinduced electron transfer of  $\text{PhCH}_2\text{SiMe}_3$  ( $4.6 \text{ kcal}$

Scheme 2



$\text{mol}^{-1}$ ).<sup>9a,54</sup> The  $k_{\text{et}}$  value agrees with both the  $k_{\text{q}}$  and  $k_{\text{obs}}$  values (Table 5). Such agreements strongly indicate that the photoaddition reaction proceeds via photoinduced electron transfer from  $\text{PhCH}_2\text{SiMe}_3$  to  $^1\text{AcrCO}^*-\text{Sc}(\text{OTf})_3$  as shown in Scheme 2. The drastically enhanced electron acceptor ability of the  $^1\text{AcrCO}^*-\text{Sc}(\text{OTf})_3$  complex as compared to  $^1\text{AcrCO}^*$  (vide supra) makes it possible for electron transfer from  $\text{PhCH}_2\text{SiMe}_3$  to  $^1\text{AcrCO}^*-\text{Sc}(\text{OTf})_3$  to occur efficiently to produce the radical ion pair ( $\text{PhCH}_2\text{SiMe}_3^{\bullet+} \text{AcrCO}^{\bullet-}-\text{Sc}(\text{OTf})_3$ ). The Si–C bond is readily cleaved by the reaction of  $\text{PhCH}_2\text{SiMe}_3^{\bullet+}$  with  $\text{AcrCO}^{\bullet-}-\text{Sc}(\text{OTf})_3$  in the radical ion pair to yield the siloxy adduct ( $k_{\text{p}}$ ) in competition with the back electron transfer from  $\text{AcrCO}^{\bullet-}-\text{Sc}(\text{OTf})_3$  to  $\text{PhCH}_2\text{SiMe}_3^{\bullet+}$ . The carbon–oxygen bond of the siloxy adduct is readily cleaved by an acid to yield the 9-benzyl-10-methylacridinium ion as the final product.

**Direct Detection of Radical Ion Intermediates.** Formation of the radical ion pair in photoinduced electron transfer from  $\text{PhCH}_2\text{SiMe}_3$  to the  $^1(1\text{-NA})^*-\text{Mg}(\text{ClO}_4)_2$  complex (Scheme 1) and the  $^1\text{AcrCO}^*-\text{Sc}(\text{OTf})_3$  complex (Scheme 2) was confirmed by the laser flash experiments. The transient absorption spectra obtained after the laser pulse excitation of the  $\text{PhCH}_2\text{SiMe}_3/1\text{-NA}-\text{Mg}(\text{ClO}_4)_2$  system are shown in Figure 7a. The transient absorption band at  $520 \text{ nm}$  in Figure 7a may correspond to the reported spectrum of  $\text{PhCH}_2\text{SiMe}_3^{\bullet+}$ , since no other possible intermediate such as  $\text{PhCH}_2^{\bullet}$  has the absorption band in this wavelength region.<sup>55,56</sup> The additional band around  $600 \text{ nm}$  may be attributed to the transient spectrum of the  $1\text{-NA}^{\bullet-}-\text{Mg}(\text{ClO}_4)_2$  complex. To confirm this assignment, a photoinduced electron transfer from a dimeric 1-benzyl-1,4-dihydronicotinamide [(BNA)<sub>2</sub>]<sup>57</sup> to the  $1\text{-NA}-\text{Mg}(\text{ClO}_4)_2$  complex was examined by means of the laser flash photolysis. The (BNA)<sub>2</sub> is

(54) The  $E^{\text{red}*}$  value ( $1.60 \text{ V}$ ) evaluated from the electrochemical measurements was used for the calculation.

(55) Fukuzumi, S.; Fujita, M.; Noura, S.; Ohkubo, K.; Suenobu, T.; Araki, Y.; Ito, O. *J. Phys. Chem. A* **2001**, *105*, 1857.

(56) The lifetime of  $\text{PhCH}_2\text{SiMe}_3^{\bullet+}$  in Figure 7 is apparently inconsistent with the large second-order rate constant of the Si–C bond cleavage of  $\text{PhCH}_2\text{SiMe}_3^{\bullet+}$  with  $\text{MeCN}$  ( $3.2 \times 10^9 \text{ M}^{-1} \text{ s}^{-1}$ ) in dichloromethane, which leads to a short lifetime of the free radical cation ( $\text{PhCH}_2\text{SiMe}_3^{\bullet+}$ ) in neat  $\text{MeCN}$  ( $<10^{-9} \text{ s}$ ).<sup>44</sup> However, the Si–C bond cleavage rate of  $\text{PhCH}_2\text{SiMe}_3^{\bullet+}$  in the cage (Scheme 2) may be much slower than the rate for the free radical cation as observed in photoinduced electron transfer from  $\text{PhCH}_2\text{SiMe}_3$  to 10-methylacridinium ion.<sup>55</sup>

(57) Patz, M.; Kuwahara, Y.; Suenobu, T.; Fukuzumi, S. *Chem. Lett.* **1997**, 567.

(49) Fukuzumi, S.; Wong, C. L.; Kochi, J. K. *J. Am. Chem. Soc.* **1980**, *102*, 2928.

(50) Ebersson, L. *Adv. Phys. Org. Chem.* **1982**, *18*, 79.

(51) (a) Marcus, R. A. *Annu. Rev. Phys. Chem.* **1964**, *15*, 155. (b) Marcus, R. A. *Angew. Chem., Int. Ed. Engl.* **1993**, *32*, 1111.

(52) When the  $\Delta G^{\ddagger}_0$  value is small such that  $\Delta G^{\ddagger}_{\text{et}} < -4\Delta G^{\ddagger}_0$ , however, eq 3 fits better with experimental results than eq 10.<sup>36</sup>

(53) The  $k_{\text{et}}$  values for the  $\text{PhCH}_2\text{SiMe}_3/\text{Mg}(\text{ClO}_4)_2$ -carbonyl systems in Table 5, calculated based on eq 10, are somewhat larger than those calculated based on eq 3 (e.g.,  $7.2 \times 10^9 \text{ M}^{-1} \text{ s}^{-1}$  for the  $\text{PhCH}_2\text{SiMe}_3/1\text{-NA}-\text{Mg}(\text{ClO}_4)_2$  system).

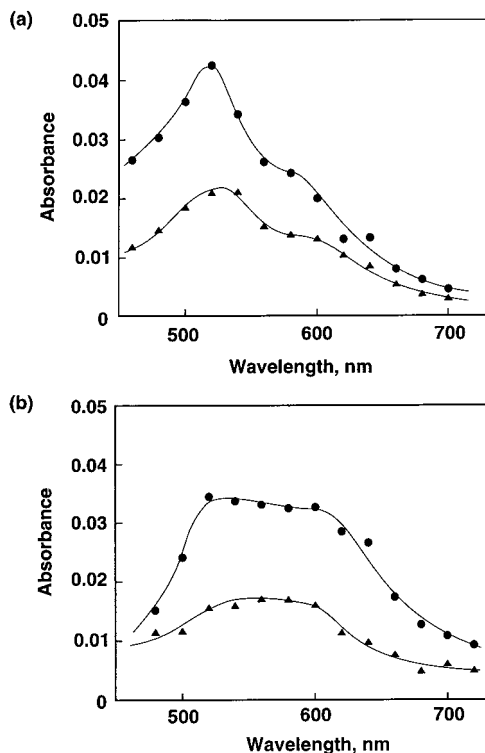
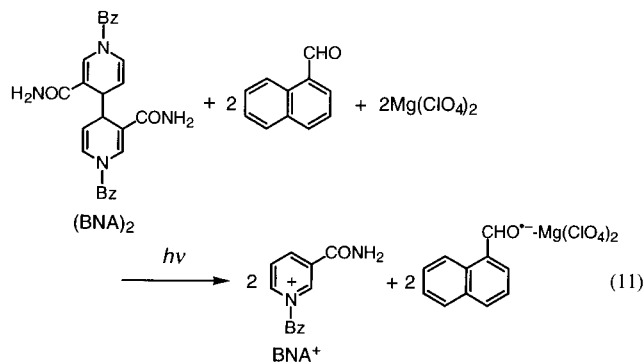


**Figure 7.** (a) Transient absorption spectra observed in the photoreaction of 1-naphthaldehyde–Mg(ClO<sub>4</sub>)<sub>2</sub> complex formed between 1-naphthaldehyde ( $2.8 \times 10^{-4}$  M) and Mg(ClO<sub>4</sub>)<sub>2</sub> (1.0 M) with PhCH<sub>2</sub>SiMe<sub>3</sub> ( $1.7 \times 10^{-1}$  M) at 1.2 (●) and 4.0 μs (▲) after laser excitation in deaerated MeCN at 298 K. (b) Transient absorption spectra observed in the photoreduction of 1-naphthaldehyde–Mg(ClO<sub>4</sub>)<sub>2</sub> complex formed between 1-naphthaldehyde ( $2.8 \times 10^{-4}$  M) and Mg(ClO<sub>4</sub>)<sub>2</sub> (1.0 M) by (BNA)<sub>2</sub> ( $2.0 \times 10^{-4}$  M) at 2.0 (●) and 12 μs (▲) after laser excitation in deaerated MeCN at 298 K.

known to act as a unique two-electron donor to produce the radical anions of electron acceptors.<sup>57,58</sup> The transient absorption spectra after the laser pulse excitation of the (BNA)<sub>2</sub>/1-NA–Mg(ClO<sub>4</sub>)<sub>2</sub> system are shown in Figure 7b, where the absorption bands at 520 and 600 nm are assigned to those of the 1-NA<sup>•-</sup>–Mg(ClO<sub>4</sub>)<sub>2</sub> complex. It has been reported that the radical cation of (BNA)<sub>2</sub> cannot be detected at the microsecond time scale due to the facile oxidation of (BNA)<sub>2</sub><sup>•+</sup>, which readily dissociates to BNA<sup>•</sup> and BNA<sup>+</sup>, then to 2 equiv of BNA<sup>+</sup>.<sup>57,58</sup> Thus, the stoichiometry of the photoinduced electron transfer from (BNA)<sub>2</sub> to the 1-NA–Mg(ClO<sub>4</sub>)<sub>2</sub> complex is given by eq 11.



Since BNA<sup>+</sup> has no absorption band in the visible region, only the radical anion part is detected in Figure 7b. Thus, the

(58) Fukuzumi, S.; Suenobu, T.; Patz, M.; Hirasaka, T.; Itoh, S.; Fujitsuka, M.; Ito, O. *J. Am. Chem. Soc.* **1998**, *120*, 8060.

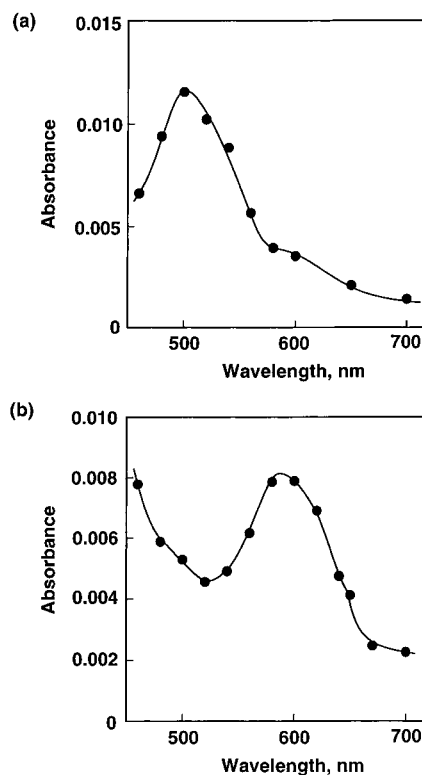


**Figure 8.** (a) Transient absorption spectra observed in the photoreduction of AcrCO–Sc(OTf)<sub>3</sub> complex formed between AcrCO ( $5.0 \times 10^{-5}$  M) and Sc(OTf)<sub>3</sub> ( $8.0 \times 10^{-2}$  M) by PhCH<sub>2</sub>SiMe<sub>3</sub> ( $2.5 \times 10^{-1}$  M) at 50 μs after laser excitation in deaerated MeCN at 298 K. (b) Transient absorption spectra observed in the photoreduction of AcrCO–Sc(OTf)<sub>3</sub> complex formed between AcrCO ( $1.0 \times 10^{-4}$  M) and Sc(OTf)<sub>3</sub> ( $4.0 \times 10^{-2}$  M) by (BNA)<sub>2</sub> ( $1.0 \times 10^{-2}$  M) at 50 μs after laser excitation in deaerated MeCN at 298 K.

absorption bands at 520 and 600 nm due to the 1-NA<sup>•-</sup>–Mg(ClO<sub>4</sub>)<sub>2</sub> complex are overlapped with the absorption band at ca. 500 nm due to PhCH<sub>2</sub>SiMe<sub>3</sub><sup>•+</sup> in Figure 7a.

The transient absorption spectrum is also obtained after the laser pulse excitation of the PhCH<sub>2</sub>SiMe<sub>3</sub>/AcrCO–Sc(OTf)<sub>3</sub> system as shown in Figure 8a. The transient absorption spectrum after the laser pulse excitation of the (BNA)<sub>2</sub>/AcrCO–Sc(OTf)<sub>3</sub> system is also shown in Figure 8b, where the absorption band at 600 nm is assigned to that of the AcrCO<sup>•-</sup>–Sc(OTf)<sub>3</sub> complex. Thus, the transient absorption spectrum in Figure 8a consists of the absorption band due to PhCH<sub>2</sub>SiMe<sub>3</sub><sup>•+</sup> at 500 nm, which is overlapped with the absorption band due to the AcrCO<sup>•-</sup>–Sc(OTf)<sub>3</sub> complex at 600 nm.

## Summary and Conclusions.

As demonstrated above, photoinduced electron transfer reactions of aromatic carbonyl compounds are remarkably accelerated by the complexation with metal ions acting as Lewis acids. A change in spin state of the lowest excited states from the triplet to the singlet is generally observed for aromatic carbonyl compounds. Photochemical redox reactions which would otherwise be unlikely to occur are allowed to proceed efficiently via Lewis acid-catalyzed photoinduced electron transfer by complexation of the photoexcited states with Lewis acids. The one-electron reduction potentials of both the ground state and excited state of aromatic carbonyl compounds are shown to be remarkably shifted to the positive direction by complexation with Lewis acids.

**Acknowledgment.** This work was partially supported by a Grant-in-Aid for Scientific Research Priority Area (Nos. 11228205 and 13031059) from the Ministry of Education, Culture, Sports, Science and Technology, Japan. Our special thanks are due to Dr. A. Ishida of Institute of Industrial Science, Osaka University for his help at the early stage of this study in the laser flash photolysis experiments and phosphorescence measurements.

**Supporting Information Available:** Experimental procedures for photochemical reactions; quantum yield determinations and laser flash photolysis (S1–S3); UV–visible spectral changes for the complex formation between AcrCO and Sc(OTf)<sub>3</sub> (S4); fluorescence decay curve of the AcrCO–Sc(OTf)<sub>3</sub> complex (S5); Stern–Volmer plots for the fluorescence quench-

ing of the Mg(ClO<sub>4</sub>)<sub>2</sub>–carbonyl complexes (S6); UV–vis spectroscopy for the photoaddition of benzyltrimethylsilane with 1-NA (S7); dependence of the quantum yield ( $\Phi$ ) on [PhCH<sub>2</sub>SiMe<sub>3</sub>] and plot of  $\Phi^{-1}$  vs [PhCH<sub>2</sub>SiMe<sub>3</sub>]<sup>-1</sup> for the photoaddition of PhCH<sub>2</sub>SiMe<sub>3</sub> with Mg(ClO<sub>4</sub>)<sub>2</sub>–carbonyl complexes (S8); dependence of the quantum yield ( $\Phi$ ) on [Me<sub>4</sub>Sn] and plot of  $\Phi^{-1}$  vs [Me<sub>4</sub>Sn]<sup>-1</sup> for the photoaddition of Me<sub>4</sub>Sn with the 1-NA–Sc(OTf)<sub>3</sub> complex (S9); dependence of the quantum yield ( $\Phi$ ) on [PhCH<sub>2</sub>SiMe<sub>3</sub>] and plot of  $\Phi^{-1}$  vs [PhCH<sub>2</sub>SiMe<sub>3</sub>]<sup>-1</sup> for the photoaddition of PhCH<sub>2</sub>SiMe<sub>3</sub> with the AcrCO–Sc(OTf)<sub>3</sub> complex (S10) (PDF). This material is available free of charge via the Internet at <http://pubs.acs.org>.

JA010125J